

CLEAN COAL TECHNOLOGY (CCT)

500 MW DEMONSTRATION OF ADVANCED
WALL-FIRED COMBUSTION TECHNIQUES
FOR THE REDUCTION OF NITROGEN OXIDE (NO_x)
EMISSIONS FROM COAL-FIRED BOILERS

CFD Modeling of SNCR Performance in
Georgia Power Company's
Hammond Unit 4 and Wansley Unit 1

DOE Contract Number
DE-FC22-90PC89651

SCS Contract Number
C-91-000027

Prepared by:

Reaction Engineering International
77 West 200 South, Suite 210
Salt Lake City, Utah 84101

Prepared for:

Southern Company Services, Inc.
600 North 18th Street
Birmingham, Alabama 35291-8195

September 1998

Cleared by DOE Patent Counsel on May 8, 1998

LEGAL NOTICE

This report was prepared by Reaction Engineering International for Southern Company Services, Inc. pursuant to a cooperative agreement partially funded by the U.S. Department of Energy and neither Southern Company Services, Inc. nor any of its subcontractors nor the U.S. Department of Energy, nor any person acting on behalf of either:

Makes any warranty or representation, express or implied with respect to the accuracy, completeness, or usefulness of the information contained in this report, or process disclosed in this report may not infringe privately-owned rights; or

Assumes any liabilities with respect to the use of, or for damages resulting from the use of, any information, apparatus, method or process disclosed in this report.

Reference herein to any specific commercial product, process, or service by trade name, trademark, manufacturer, or otherwise, does not necessarily constitute or imply its endorsement, recommendation, or favoring by the U.S. Department of Energy. The views and opinion of authors expressed herein do not necessarily state or reflect those of the U.S. Department of Energy.

CFD Modeling of SNCR Performance in Georgia Power Company's Hammond Unit 4 and Wansley Unit 1

**A Final report prepared for Southern Company Services
by
Reaction Engineering International**

Authors: M.A. Cremer and E.G. Eddings

September 1998

CONTENTS

1.0 EXECUTIVE SUMMARY	1
2.0 INTRODUCTION AND OBJECTIVES	4
3.0 SELECTIVE NON-CATALYTIC REDUCTION	5
4.0 PROGRAM ORGANIZATION AND APPROACH.....	7
Field Measurements	8
Physical Cold Flow Modeling.....	9
5.0 CFD MODELING.....	11
Overall Approach to Modeling SNCR.....	11
Model Description.....	11
SNCR Chemistry.....	13
Furnace Model	13
Model Assumptions	14
6.0 MODEL PREDICTIONS	16
Hammond Unit 4	16
Lower Furnace Results	16
Injection Strategies	16
Results	19
Convective Pass Injection (Fully-Mixed Cases).....	21
High-Energy Anhydrous Ammonia Injection.....	22
Low-Energy Aqueous Urea Injection	27
Spatially Dependent Inlet NO _x Distribution.....	29
Summary of Hammond Unit 4 Predictions	36
Wansley Unit 1	37
Lower Furnace Simulation	37
Injection Strategies	38
Results	40
Convective Pass Injection (Fully-Mixed Cases).....	42
High-Energy Anhydrous Ammonia Injection	45
Aqueous Urea Injection	51
Summary of Wansley Unit 1 Predictions	59
7.0 CONCLUSIONS	60
8.0 REFERENCES	61

LIST OF FIGURES

Figure 4-1 Flow diagram for program to evaluate large-scale SNCR performance	7
Figure 4-2 Schematics showing measurement locations used in boiler tests	8
Figure 6-1 Predicted temperature distribution in the lower furnace of Hammond Unit 4 ...	17
Figure 6-2 Schematic of Hammond Unit 4 upper furnace geometry indicating the injection strategies that were modeled	19
Figure 6-3 The inlet flue-gas temperature for the upper furnace geometry was obtained by interpolation from the lower furnace simulation	20
Figure 6-4 Comparison of measured temperatures in upper furnace of Hammond Unit 4 with scaled and unscaled predicted temperatures	21
Figure 6-5 Predicted temperature distribution in the upper furnace of Hammond Unit 4 ...	22
Figure 6-6 Schematic showing placement of injection nozzles for Hammond Case 3	23
Figure 6-7 Predicted NOx distribution in Hammond Unit 4 for Case 3	23
Figure 6-8 Schematic showing placement of nozzles in Hammond Unit 4 for Case 4	24
Figure 6-9 Predicted NOx distribution in Hammond Unit 4 for Case 4	25
Figure 6-10 Injection strategy for Hammond Case 5	26
Figure 6-11 Schematic showing placement of nozzles in Hammond Case 6	27
Figure 6-12 Predicted mixture fraction and NOx distribution for Hammond Case 6	28
Figure 6-13 Schematic showing placement of injectors for Hammond Case 7	29
Figure 6-14 Predicted mixture fraction and NOx distribution for Hammond Case 7	30
Figure 6-15 Schematic case 8 injection strategy for Hammond Unit 4	31
Figure 6-16 Comparison of jet penetration in Case 6	32
Figure 6-17 Comparison of reagent distribution between Case 8 and Case 6	33
Figure 6-18 Predicted NOx distribution for Hammond Case 8	34
Figure 6-19 Predicted NOx distribution in Hammond Case 6	35
Figure 6-20 Computed lower furnace temperature distribution for Wansley Unit 1	37
Figure 6-21 Comparison between computed lower furnace properties with interpolated properties at the inlet to the upper furnace for the simulation of Wansley Unit	38
Figure 6-22 Comparison between measured and predicted gas temperatures in Wansley Unit 1	39

Figure 6-23 Schematic of upper furnace geometry and injection strategies considered in the CFD simulations of Wansley Unit 1	41
Figure 6-24 Predicted upper furnace temperature distribution for Wansley Unit 1	42
Figure 6-25 Schematic for Wansley Cases 1 and 2 showing location of uniform reagent injection planes	43
Figure 6-26 Predicted upper furnace temperature and NO _x concentration profiles in Wansley Unit 1 Case 1	44
Figure 6-27 Convective pass injection strategy for Wansley Case 3	45
Figure 6-28 Predicted NO _x and NH ₃ distribution for Wansley Case 3	46
Figure 6-29 Schematic showing injection strategy for Wansley Case 4	47
Figure 6-30 Predicted temperature and NO _x distribution in Wansley Case 4.....	48
Figure 6-31 Schematic showing injection strategy for Wansley Case 5	49
Figure 6-32 Predicted NO _x distribution for Wansley Case 5	50
Figure 6-33 Injection strategy for Wansley Case 6.....	51
Figure 6-34 Predicted gas temperature and urea products distribution for Wansley Case 6.....	52
Figure 6-35 Gas phase urea products and water vapor from droplets in the plane of two injectors for Wansley Case 6	53
Figure 6-36 Predicted NO _x distribution in the upper furnace for Wansley Case 6	54
Figure 6-37 Injection strategy for Wansley Case 7.....	55
Figure 6-38 Predicted distribution of urea gas phase products and mean droplet trajectories for four droplet sizes for Wansley Case 7.....	56
Figure 6-39 Mass fraction of urea gas phase products for Wansley Case 7	57
Figure 6-40 Predicted NO _x distribution for Wansley Case 7	58

LIST OF TABLES

Table 4-1 Summary of HVT Temperature Measurements- Georgia Power Plant Wansley Unit 1	9
Table 4-2 Summary of HVT Temperature Measurements- Georgia Power Plant Hammond Unit 4	10
Table 5-1 Reaction Steps in Reduced SNCR Mechanism	14
Table 6-1 Summary of Injection Strategies for Hammond Unit 4	18
Table 6-2 Predicted NOx Reduction and NH3 Slip for Hammond Unit 4	20
Table 6-3 Summary of Injection Strategies for Wansley Unit 1	40
Table 6-4 Predicted NOx Reduction and NH3 Slip for Wansley Unit 1	41

1.0 EXECUTIVE SUMMARY

Regulatory agencies, consultants and utilities (SAIC, 1996; ICAC, 1994) have made assumptions regarding the NO_x reduction capabilities of selective non-catalytic reduction (SNCR) on large coal-fired boilers. Generally, these assumptions are based on the extrapolation of performance data from relatively successful experience with SNCR on smaller boilers (<165 MW). However, larger boilers have physical characteristics that may hamper the successful application of SNCR.

This report discusses the results of a program to investigate the potential performance of SNCR on two large pulverized coal-fired boilers. The two units evaluated were Georgia Power Company's Hammond Unit 4, located in Rome, Georgia and Wansley Unit 1, located in Ropoville, Georgia. These two boilers are examples of units that could be affected by more stringent ozone attainment regulations that would require NO_x controls beyond low-NO_x combustion technologies. Hammond Unit 4 is a wall-fired 500 MW Foster Wheeler unit that has been retrofitted with Foster Wheeler low-NO_x burners and overfire air. Wansley Unit 1 is a twin-furnace, tangentially fired 880 MW Combustion Engineering unit that has been retrofitted with ABB C-E Services' Low-NO_x Concentric Firing System Level 2.

1.1 Selective Non-catalytic Reduction

In concept, the SNCR process is simple. Ammonia (anhydrous or aqueous) or urea (aqueous) is injected and mixed into the flue gas of a boiler in a limited temperature range (1600 to 2100°F). The injected reagent then reacts selectively with NO_x to form N₂ and H₂O. Introducing the reagent at temperatures that are too high can degrade performance because the reducing agent is oxidized and little or no NO_x reduction occurs. Further, at lower temperatures the reduction reactions are too slow and unreacted reagent "slips" through the process. On small coal-fired units (<165 MW), SNCR has demonstrated NO_x reduction capabilities ranging from 25 to 45 percent under normal load dispatch conditions with tolerable levels of ammonia slip. This variation in NO_x reduction capability depends on site-specific considerations and the amount of ammonia slip that is considered tolerable.

For large boilers, there are a number of challenges associated with applying SNCR. In particular, the large physical dimensions pose challenges for injection and mixing the chemical with the flue gas. Another issue with larger units is the fact that the SNCR temperature window often exists within the convective passes. Demonstrations to date at Port Jefferson, Morro Bay and Merrimac have shown that injecting only in the convective pass can create high ammonia slip due to limited residence time. Combining convective pass injection with radiant furnace injection can be an effective approach, however.

1.2 Program Organization and Approach

A three component program was used to assess potential performance of SNCR on the Hammond and Wansley boilers. First, field measurements, including furnace exit gas temperatures and emissions characteristics, were conducted to determine the existing performance conditions of the boiler. Second, physical cold flow models of the boilers were

used to assess the mixing characteristics of a number of reagent injection strategies. Finally, computational fluid dynamics (CFD) modeling was utilized to evaluate the most promising injection strategies that were identified as part of the physical modeling study. The focus of the effort was to assess the performance potential of SNCR at full load under steady state operating conditions assuming base load operations. The focus of this report is the CFD modeling results.

1.3 CFD Modeling

The computational tools used during this program simulate reacting and nonreacting flow of gases and particles. *BANFF* is Reaction Engineering International's (REI) three-dimensional, gas-phase turbulent reacting flow code, and *GLACIER* adds physical models to treat two-phase flows. *BANFF* and *GLACIER* are both steady state three-dimensional CFD codes that fully couple reacting gases, solids and liquids with turbulent mixing and radiative heat transfer. Coupling turbulence and heat transfer with finite-rate reaction chemistry requires the number of chemical kinetic steps to be relatively small. *BANFF* and *GLACIER* use assumptions of partial equilibrium and steady state species to compute local finite-rate chemistry using a set of reduced kinetic steps for slow reactions and minimize Gibbs free energy for all other species. A reduced set of seven SNCR reactions is coupled into *BANFF* and *GLACIER* (Brouwer, et al., 1996) to model finite-rate chemistry associated with SNCR.

1.4 Results

The field measurements and the physical cold flow modeling results were used to limit the number of injection strategies to consider with the CFD modeling. For the wall-fired unit equipped with low-NO_x burners and overfire air (Hammond 4), over 20 configurations were evaluated with physical cold flow modeling. Out of these, eight injection scenarios were evaluated using CFD. For the cases modeled, the CFD results showed that SNCR has the potential to reduce NO_x emissions at full load by 30-35 percent while maintaining ammonia slip below 5 ppm. Of the configurations evaluated, the most promising scenario involved the injection of ammonia (NH₃/NO = 1.0) via a row of high-energy wall injectors located on the front wall 14 feet above the boiler nose (Figure 6-11).

For the tangentially fired unit equipped with a low-NO_x concentric firing system (Wansley 1), fifteen injection configurations were evaluated with physical cold flow modeling. Out of these, seven injection scenarios were evaluated with CFD. For the cases modeled, the CFD results showed that SNCR has the potential to reduce NO_x emissions by 20-25 percent with an ammonia slip of less than 10 ppm. The most promising scenario involved the injection of aqueous urea via high-energy wall injectors located on the front wall 29 feet above the nose. The firing characteristics of this boiler (supercritical, separated overfire air, eastern bituminous fuel, 8 corner) and access limitations not permitting lances in the convective pass make achieving higher levels of NO_x reduction more difficult.

The SNCR systems evaluated in this program were designed for full load steady state operations only. It should also be noted that there was no effort to optimize each injection scenario by biasing reagent flow to each injector. In an actual installation, this biasing would

be a necessary step to optimize SNCR performance. In addition, the site specific nature of SNCR demands caution in applying these results to day-to-day operations of other boilers having various boiler duty cycles and swinging loads.

2.0 INTRODUCTION AND OBJECTIVES

Regulatory agencies, consultants, and utilities (SAIC, 1996; ICAC, 1994) have made assumptions regarding the NO_x reduction capabilities of selective non-catalytic reduction (SNCR) on large coal-fired boilers. Generally, these assumptions are based on the extrapolation of performance data from relatively successful experience with SNCR on smaller boilers (<165 MW). However, larger boilers have physical characteristics that may hamper the successful application of SNCR. These include limited access to appropriate temperature regions in the boiler, greater asymmetry in combustion temperatures and velocity profiles, and longer distances over which reagent must be delivered and mixed in the boiler.

To address this issue, the U.S. Department of Energy (DOE), the Electric Power Research Institute (EPRI), and Southern Company Services (SCS) have funded a program to evaluate the performance of SNCR in large-scale coal-fired boilers. The two boilers selected for evaluation were Georgia Power Company's Hammond Unit 4, located in Rome, Georgia and Wansley Unit 1, located in Roopville, Georgia. These two boilers are examples of units that could be affected by more stringent ozone attainment regulations that would require NO_x controls beyond low-NO_x combustion technologies. To address SNCR performance, this program consisted of three components: 1) field measurements, 2) physical cold flow modeling, and 3) computational fluid dynamics (CFD) modeling. This report focuses on a discussion of the results of the CFD modeling portion of the program.

This report is organized as follows. The following two sections provide some preliminary discussion. Section 3.0 gives a brief description of selective non-catalytic reduction (SNCR) and some of the issues involved in its application to large coal-fired boilers. Section 4.0 is a brief discussion of the program organization and the interaction between the program components. The remainder of the report presents a discussion of the CFD modeling that was conducted in this program to evaluate the performance of SNCR in Hammond Unit 4 and Wansley Unit 1.

3.0 SELECTIVE NON-CATALYTIC REDUCTION

In concept, the SNCR process is simple. Ammonia (anhydrous or aqueous) or urea (aqueous) is injected and mixed into the flue gas of a boiler in a limited temperature range (1600 to 2100°F). The injected reagent then reacts selectively with NO_x to form N₂ and H₂O. Introducing the reagent at temperatures that are too high can degrade performance because the reducing agent is oxidized and little or no NO_x reduction occurs. Further, at lower temperatures the reduction reactions are too slow and unreacted reagent “slips” through the process. On small coal-fired units (<165 MW), SNCR has demonstrated NO_x reduction capabilities ranging from 25 to 45 percent under normal load dispatch conditions with tolerable levels of ammonia slip. This variation in NO_x reduction capability depends on site-specific considerations and the amount of ammonia slip that is considered tolerable.

In practical applications, the SNCR process can be complicated. Non-uniformities in velocity and temperature at the reagent injection location can pose operational difficulties because of the inherent sensitivity of the process to these parameters. The physical location within the boiler of the effective temperature range changes depending on operating factors such as unit load, fuel type, soot blowing cycles, mill patterns, etc. Generally, these factors require the utilization of multiple injection elevations in full-scale systems, especially for those boilers operated with a cycling load profile. There are also other balance-of-plant issues involved in the use of SNCR including: 1) ammonia contamination of fly-ash, 2) air heater pluggage in regions of high ammonia slip, 3) formation of ammonium chloride plumes, and 4) the emission or production of undesirable by-products of the SNCR process, such as NH₃, CO, or N₂O. These are concerns that must be considered in the application of SNCR.

Commercial SNCR systems may be categorized in two ways: 1) by the type of reagent used (i.e. ammonia or urea-based); and 2) by the type of injection system used (i.e., low-energy or high-energy). A low-energy system utilizes pressure or dual fuel atomizers to inject chemical from the furnace walls or from water-cooled lances. For these systems, furnace turbulence and the ballistic trajectory of the injected chemical control mixing. Low-energy systems are only appropriate for aqueous reagent injection, in particular, aqueous urea. High-energy systems utilize a larger quantity of either steam or air to inject chemical (on the order of 1 to 2 percent of the boiler flue gas flow). In this case the energy for mixing is provided by the momentum of the injected flow, and either urea or ammonia (anhydrous or aqueous) may be used.

For large boilers, there are a number of challenges associated with applying SNCR. For example, if a low-energy system is used with injectors at the boiler wall, there is the question of having sufficient momentum for the spray to adequately mix with the flue gas. If water-cooled lances are used to extend low-energy injectors into the flue gas, there is the question of how long to make the lances to provide necessary mixing, and whether there is enough cooling flow through the lances to avoid mechanical failure. The same questions also apply to high-energy systems, although the jet penetration scales better with size. Another issue with larger units is the fact that the SNCR temperature window often exists within the convective passes. Demonstrations to date at Port Jefferson, Morro Bay, and Merrimac have shown that injecting only in the convective pass can create high ammonia slip due to limited residence

time. However, when combined with radiant furnace injection, overall SNCR performance can be improved over radiant furnace or convective pass injection only (Lin, 1992; Shore, 1993).

4.0 PROGRAM ORGANIZATION AND APPROACH

A three component program, illustrated in Fig. 4-1, was used to assess performance of SNCR on the Hammond and Wansley boilers. First, field measurements including furnace exit gas temperatures and emissions characteristics were conducted to determine the existing performance conditions of the boiler. Second, physical cold flow models of the boilers were constructed and tested to assess the mixing characteristics of a number of reagent injection strategies. Finally, computational fluid dynamics (CFD) modeling was utilized to evaluate the most promising injection strategies that were identified as part of the physical modeling study.

While a number of different perturbations of SNCR injection strategies could have been evaluated as part of this study, the focus of this effort was to assess the performance potential of SNCR at full load under steady state operating conditions assuming base load operations. The impact of flue gas temperature and/or velocity profile changes caused by different excess air levels, slag buildup in the furnace, soot blowing, reduced load, cycling load profiles, varying burner-in-service strategies, and/or fuel types were not investigated. These different operating conditions will result in varying performance levels for the SNCR systems evaluated herein, and most certainly would require that the system design be more robust and flexible to handle the performance challenges these impacts create.

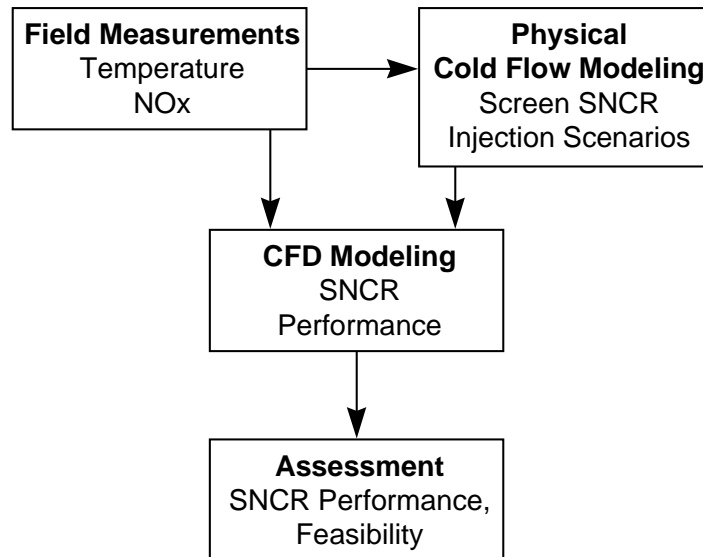
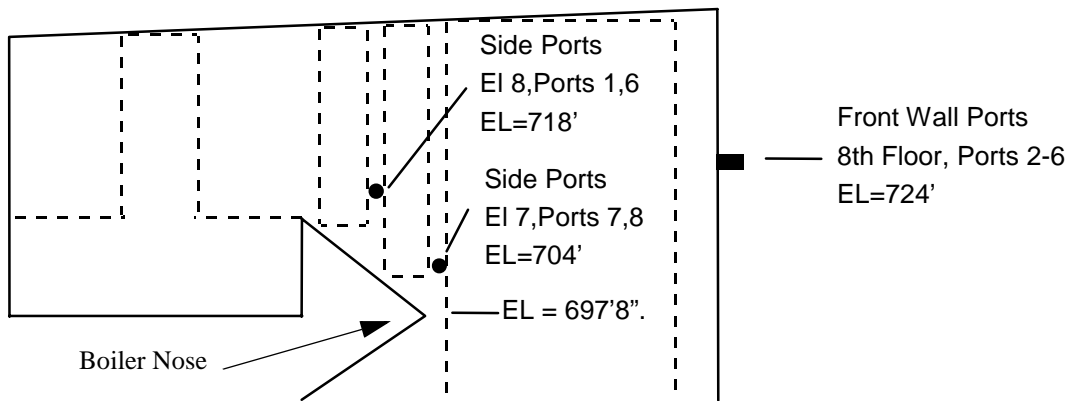


Figure 4-1: Flow diagram for program to evaluate large-scale SNCR performance

4.1 Field Measurements

Although only the full load data were used in this study, temperature and emissions measurements were collected at various loads and operating conditions. At Plant Wansley, data were gathered at loads of 880, 650, and 450 MW. Tests were performed at 880 MW using coals with different slagging tendencies: a Kerr McGee coal and a Lone Mountain/Pardee blend. The data collected while firing the 1.1% sulfur Kerr McGee coal (6.5% ash, 10.3% moisture, 31.4% volatiles, 51.8% fixed carbon) were used for the modeling studies. Suction pyrometry, utilizing high velocity thermocouple (HVT) probes, was used to collect the furnace temperature data. [The HVT measurement locations are shown in Figure 4-2.] NO,

a)



b)

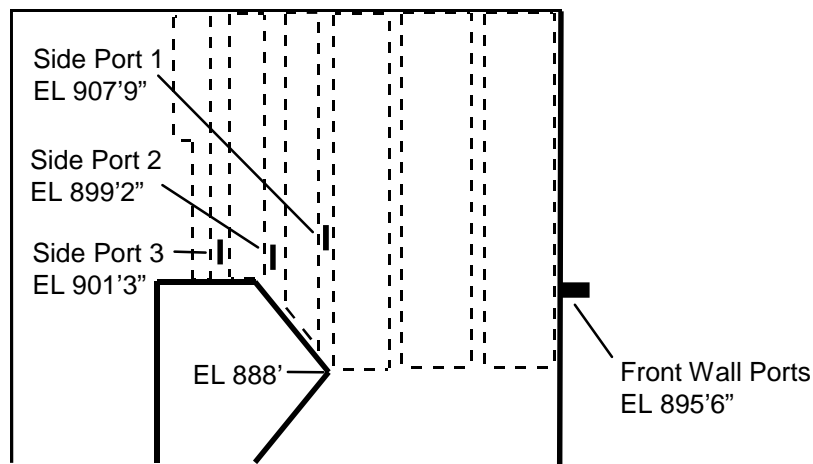


Figure 4-2: Schematics showing measurement locations used in boiler tests. a) Hammond Unit 4. b) Wansley Unit 1.

O₂, and CO measurements were made at the same location as the temperature measurements and were supplemented by data from the continuous emissions monitoring system and the control room. Table 4-1 summarizes the results of the temperature measurements performed during this program. These data show that the furnace exit gas temperatures, which averaged in excess of 2340°F, were all too hot for effective SNCR operation in those regions.

Table 4-1: Summary of HVT Temperature Measurements Georgia Power Plant Wansley Unit 1

Load (MW) and Coal	Test Location	Temperature (°F)		
		Range	Average	Std. Dev.
880 Kerr McGee	Front Wall (Exit)	2300-2588	2452	74
	Side Port 1	1969-2237	2129	--
880 Lone Mountain and Pardee Blend	Front Wall (Exit)	2269-2610	2442	90
	Side Port 1	2116-2167	2149	--
	Side Port 2	1872-1976	1923	--
	Side Port 3	1825-1886	1850	--
653 Lone Mountain	Front Wall (Exit)	2307-2545	2448	63
	Side Port 1	2048-2250	2155	--
	Side Port 2	1836-1947	1896	--
	Side Port 3	--	--	--
450 Kerr McGee and Lone Mountain/ Pardee Blend	Front Wall (Exit)	1990-2484	2347	99
	Side Port 1	1868-2160	2052	--
	Side Port 2	1724-1893	1837	--
	Side Port 3	--	--	--

Tests were also performed at Plant Hammond Unit 4 at loads of 480, 400 and 300 MW using a 1.7% sulfur eastern bituminous coal (9.1% ash, 6.1% moisture, 33.1% volatiles, 51.7% fixed carbon). In addition to the HVT temperature measurements, O₂ measurements were made at the same locations. Table 4-2 summarizes the results of the temperature measurements and Figure 4-2 shows the locations where the measurements were taken. The data show that temperatures measured at the furnace exit (front wall measurements) were within the desired urea SNCR temperature range at loads of 400 MW and higher. Temperatures behind the superheat pendants (El. 8, Ports 1 and 6) were too cold for all test conditions. Conversely, temperatures at the furnace nose (El. 7, Ports 7 and 8) were above the desired temperature range for all test conditions.

4.2 Physical Cold Flow Modeling

Physical cold flow modeling was used to screen possible SNCR injection scenarios for both Hammond Unit 4 and Wansley Unit 1, ultimately limiting the number of cases investigated during the CFD modeling phase of the program. Although not capable of simulating temperature effects, physical modeling provided a method for quickly screening the mixing performance of different injection configurations. Velocity and tracer gas measurements were

Table 4-2: Summary of HVT Temperature Measurements Georgia Power Plant Hammond Unit 4

Load (MW)	Test Location	Temperature (°F)		
		Range	Average	Std. Dev.
480	Furn. Exit (El 8)	1450-2472	1939	202
	El 8, Ports 1,6	1520-2003	1799	105
	El 7, Ports 7,8	1813-2472	2202	143
400	Furn Exit (El 8)	1460-2232	1881	176
	El 8, Ports 1,6	1375-2063	1784	162
	El 7, Ports 7,8	1885-2472	2230	136
300	Furn. Exit (El 8)	1325-2018	1759	158
	El 8, Ports 1,6	1262-1740	1544	133
	El 7, Ports 7,8	1817-2404	2143	146

used to quantitatively define mixing performance in the 1:24 scale models. Over 20 configurations were evaluated for the Hammond model, with an additional 15 for the Wansley model. These configurations were narrowed to a few optimal mixing cases, which were then modeled using CFD.

For both the Hammond and Wansley boilers, the physical cold flow modeling work indicated that high-energy injection, in general, achieved better mixing of reagent than low-energy injection. In the Hammond boiler, the five division panels extending from the front wall in the lower furnace up to the roof reduced the length scale of the largest turbulent eddies in the upper furnace to the distance between the panels. The four large superheater pendants in the Wansley unit had the same effect. This reduction in the turbulence length scales tends to reduce the degree of advection of reagent away from the wall so that jet penetration into the furnace becomes more important. The panels also presented a barrier to lateral mixing in the upper furnace. For a constant overall mass flowrate of injected reagent, the cold flow modeling indicated that the use of a single injector centered between the division panels or superheater pendants achieved better mixing than did multiple injectors.

5.0 CFD MODELING

5.1 Overall Approach to Modeling SNCR

In practical combustion systems, NO_x reduction efficiencies are primarily dependent on three factors: 1) mixing, 2) temperature, and 3) residence time. Efficiencies increase when all three act in concert such that the reagent is fully mixed with the flue gas at optimum temperatures over a sufficient residence time. In practical combustion systems, severe design constraints are placed on the reagent injection system which must disperse the reagent throughout the entire combustion product stream while the gases are within the appropriate temperature window. The spatial location of the optimum temperature window varies with operating conditions and may occur in regions of large thermal gradients. In addition, control of the SNCR system can be problematic due to the lack of directly measurable variables for accurate feedback and/or feed forward control and trim signals. Thus, the design of SNCR injection systems requires an analysis capability that takes into account the nonlinear coupling between these physical processes. Accurate representation of mixing, temperature, and residence times requires analysis of and coupling between turbulent fluid mechanics, radiative and convective heat transfer, spray droplet evaporation, particle decomposition, and gas phase chemistry. The CFD tools used in this program include the capability to model this level of coupling.

5.2 Model Description

The computational tools used by Reaction Engineering International (REI) are based on software developed over the last two decades by Dr. Philip J. Smith, vice president of REI, and his students and colleagues at the University of Utah and REI. The current software simulates reacting and nonreacting flow of gases and particles, including gaseous diffusion flames, pulverized-coal flames, liquid sprays, coal slurries, isothermal and reacting two-phase flows, injected sorbents, and other oxidation/reduction systems. BANFF is REI's three-dimensional, gas-phase turbulent reacting flow code, and GLACIER adds physical models to treat two-phase flows. These software tools have been applied to a wide variety of industrial systems encompassing utility boilers, pyrolysis furnaces, gas turbine combustors, rotary kilns, waste incinerators, smelting cyclones and others. These applications have been used for basic design, problem solving, pollution control, etc. using many different fuels including natural gas, coal, and waste.

The computational approach involves numerical discretization of the partial differential equation set which describes the physics of the system, including equations for conservation of mass, momentum, and energy. Typically 10^5 - 10^6 discrete computational nodes are needed to resolve the most relevant features of a three-dimensional combustion process. Around 60 variables (representing, e.g., gas velocity, temperature, concentration of various chemical species) are tracked at each node. Accurate simulation of the combustion processes requires accurate modeling of the dominant or controlling physical mechanisms in the process. Simulation of the SNCR process in a coal-fired boiler requires modeling of the flow patterns, reaction chemistry for heat release as well as NO_x and SNCR reagents, gas and wall temperatures, and heat transfer in the furnace. In the computer model used here, coupled

equations of chemical reaction, turbulent fluid flow and mixing, and convective and radiative heat transfer are solved to give a realistic and detailed model of the processes taking place within the boiler.

Turbulence can be modeled using various traditional methods of moment closure including Prandtl's mixing length model, the two-equation k- ϵ model (Launder and Spalding, 1972) and the nonlinear k- ϵ model (Speziale, 1987). In all simulations discussed in this report, the standard k- ϵ model was used due to its general applicability in modeling the mean velocity field in reacting flows.

Within the model, the rate at which the primary combustion reactions occur is assumed to be limited by the rate of mixing between the fuel and the oxidizer. That is, the rate of chemical reactions is assumed to be fast compared to the rate of mixing (i.e. full chemical equilibrium is assumed), which is a reasonable assumption for the chemical reactions governing heat release. So, the thermochemical state at each spatial position is a function of the degree of mixing (parametrized by the mixture fraction, f), the mass fraction of coal particle off-gas (η), and the enthalpy (parametrized by the degree of heat loss, H). The effect of turbulence on mean chemical composition is incorporated by assuming that the mixture fraction, obtained using the k- ϵ model, is described by a "clipped-gaussian" probability density function having spatially varying mean \bar{f} , and variance g . Mean chemical species concentrations are obtained by convolution over this assumed probability density function (PDF). Chemical reactions that are kinetically controlled, such as those involved in SNCR, are handled differently to account for turbulence-chemistry interactions. This is discussed in section 5.3.

Particle-phase mechanics are solved by following the mean path or trajectory for a discretized group or ensemble of particles in a Lagrangian frame of reference. Particle mass and momentum sources are converted from a Lagrangian to an Eulerian reference frame where they are coupled with gas phase fluid mechanics. The dispersion of the particle cloud is based on statistics gathered from the turbulent flow field. Heat, mass, and momentum transport effects are included for each particle cloud.

Particle reaction processes include coal devolatilization, char oxidation and gas-particle interchange. Particle swelling is accounted for empirically. The particles are assumed to be isothermal. Particle reaction rates are characterized by multiple parallel reaction rates with fixed activation energies. The parameters which describe the particle reaction rates are part of the input to the code. Particles are defined to consist of coal, char, ash and moisture. Ash is inert by definition; volatile mineral matter is considered as part of the volatile matter of the coal. The offgas from particle reactions is assumed to be of constant elemental composition. Turbulent fluctuations and complete, local, complex chemical equilibrium are included in the particle reactions.

Since radiation is typically the most significant mode of heat transfer in a large boiler, it is critical that the radiation field be accurately represented. Accurately simulating radiative transfer to specific regions in a system requires a model which can account for both absorbing-emitting radiation processes and complex system geometries, including arbitrary structures such as convective tube passes. Additionally, it is desirable that any radiative model

selected be computationally efficient in terms of execution time and storage to allow coupling with other routines in a comprehensive combustion model. REI's model utilizes the discrete-ordinates method which has been shown to be a viable choice for modeling radiation in combustion systems, both in terms of computational efficiency and accuracy. This method retains the directional dependency of the radiation intensity in a way that other flux models are unable to achieve, yet provides for a finite-difference or finite-volume solution that is more computationally efficient than zone methods and more deterministic than Monte Carlo methods. The development of the discrete-ordinates method and its application to a number of complex geometries (e.g., Adams, 1993; Adams and Smith, 1993) have been presented in the literature and serve to validate the use of this method in accurately modeling radiative heat transfer in coal-fired boilers (Adams, 1993; Adams & Smith, 1993; Adams & Smith, 1995).

5.3 SNCR Chemistry

BANFF and GLACIER are both steady state three-dimensional CFD codes that fully couple reacting gases, solids, and liquids with turbulent mixing and radiative heat transfer. Coupling turbulence and heat transfer with finite-rate reaction chemistry requires the number of chemical kinetic steps be relatively small. BANFF and GLACIER use assumptions of partial equilibrium and steady state species to compute local finite-rate chemistry using a set of reduced kinetic steps for slow reactions and minimize Gibbs free energy for all other species. Mean species concentrations, density, and temperature are calculated using an assumed PDF approach. One important difference between this model and other CFD-based SNCR models is that the SNCR chemistry is incorporated and fully coupled into the CFD calculation.

The reduced SNCR mechanism implemented into BANFF and GLACIER was developed previously by Brouwer, et al. (Brouwer, et al. 1996). It is based on the kinetic rates of Miller and Bowman (1989) with recent literature modifications (Dean, et al. 1991). The reduced mechanism was derived from the detailed mechanism through sensitivity analyses and curve fitting. The reduced set of seven reaction steps are given in Table 5-1. The SNCR reaction chemistry includes tracking of NO, NH₃, and HNCO concentrations as well as NCO and N₂O.

5.4 Furnace Model

The numerical solution of the governing equations of mass, momentum, and energy that are used to describe the physics of the turbulent reacting flow in a utility boiler requires the subdivision of the entire domain into tiny cubes or "cells". The numerical method involves discretization of the governing equations involving differences in properties between neighboring cells. Accurate representation of large spatial gradients in properties requires that the spacing between the cells be small to minimize error associated with the discretization. Since gradients in velocity, temperature, and species concentrations can be quite large in the vicinity of inlet or burner regions, grid resolution (cell spacing) must be relatively small, requiring many cells to accurately represent flow and scalar properties in the region of a single burner. Coal-fired utility boilers commonly have tens of burners in addition to other inlets such as close-coupled or separated overfire air ports each requiring a significant level of grid resolution. In addition to the resolution requirements in the lower furnace, SNCR reagent injectors in the upper furnace impose even more severe resolution requirements. Injector

Table 5-1:Rate parameters for the Reduced SNCR Mechanism

Reaction	A	b	E _a
1a. $NH_3 + NO \rightarrow N_2 + H_2O + H$ (T<1900°F)	1.12	5.3	37,450
1b. $NH_3 + NO \rightarrow N_2 + H_2O + H$ (T>1900°F)	1.68E-05	5.3	8,552
2a. $NH_3 + O_2 \rightarrow NO + H_2O + H$ (T<1900°F)	1.90E-01	7.65	95,253
2b. $NH_3 + O_2 \rightarrow NO + H_2O + H$ (T>1900°F)	5.97E-11	7.65	37,120
3. $HNCO + M \rightarrow H + NCO + M$	2.40E+14	0.85	68,000
4. $NCO + NO \rightarrow N_2O + CO$	1.00E+13	0.00	-390
5. $NCO + OH \rightarrow NO + CO + H$	1.00E+13	0.00	0
6. $N_2O + OH \rightarrow N_2 + O_2 + H$	2.00E+12	0.00	10,000
7. $N_2O + M \rightarrow N_2 + O + M$	6.90E+23	-2.50	64,760
Units are A=cm-mol-s-K; E _a =cal/mol			

diameters are as small as 1 inch while utility boilers can be over 120 feet in height. This wide range of length scales imposes severe grid resolution requirements on the CFD model. While boiler simulations encompassing 600,000-700,000 nodes are now relatively commonplace, an SNCR model which couples both upper furnace and lower furnace computations would easily be twice this size. Although conceivable with present computing capability, a model of this size becomes infeasible in view of the imposed time constraints of completing several parametric studies within a reasonable time period.

A technically feasible approach to address the issues of this program within a reasonable time frame is to decouple the upper and lower furnace simulations. Since the parametric studies were limited to the examination of effects of SNCR injection strategies within the upper furnace, the assumption that these changes have no significant effect on lower furnace conditions is acceptable. The approach that was followed in this program was to impose the same set of outlet conditions from the lower furnace simulation as inputs to each upper furnace simulation. The simulation of the Hammond and Wansley boilers required a three-step process: 1) simulation of the lower furnace properties (up to or past the nose), 2) interpolation of the velocity and temperature fields from the lower furnace simulation onto the inlet of the upper furnace grid, and 3) simulation of the upper furnace properties.

5.5 Model Assumptions

Aside from the general modeling assumptions that are built into the REI models (discussed in section 5.2), there are some specific assumptions that were made in the upper furnace simulations arising from decoupling the lower and upper furnace simulations. The spatial distribution of velocity and temperature was specifically represented in the inlet conditions for the upper furnace computations. These distributions were interpolated from the results of the

lower furnace as discussed previously. The flue-gas composition exiting the lower furnace was represented using an average composition, although the variable temperature imposes variability in the inlet composition through assumption of local chemical equilibrium. However, variability in the inlet flue gas composition due to lower furnace mixing limitations is not explicitly accounted for. The spatial distribution of NO_x concentration at the nose of the boilers was assumed to be uniform in the majority of the simulations. However, the effect of this particular approximation on the resulting predictions of NO_x was determined to have only a second-order effect. These predictions are discussed in Section 6.0.

6.0 MODEL PREDICTIONS

6.1 Hammond Unit 4

Hammond Unit 4 utilizes a wall-fired 500 MW Foster Wheeler boiler that has been retrofitted with Foster Wheeler controlled-flow/split-flame low-NO_x burners and an advanced overfire air system. The boiler has design steam conditions of 2500 psig and 1000/1000^oF superheat/reheat temperatures, respectively. It is a balanced draft unit with two forced draft and three induced draft fans. The flue gases exit the economizer through two Ljungstrom air preheaters and into the cold side ESP, then through the induced draft fans and finally out to the stack. The furnace cross-section measures nominally 52.5 feet wide and 40 feet deep. This boiler is similar to other Foster Wheeler boilers built during the same period. However, this unit is equipped with overfire air. As a result, its combustion characteristics may not be typical of other Foster Wheeler units equipped with low-NO_x burners only.

6.1.1 Lower Furnace Results

Hammond Unit 4 was previously modeled as part of a program funded by the Electric Power Research Institute (EPRI) and the U.S. Department of Energy (DOE) (Eddings, et al., 1997). From this study, one set of simulation results typical of firing at full load (480 MW) was used to supply the necessary input information for the current work. This case was representative of conditions existing during one of the test points (test #115) of the Innovative Clean Coal Technology (ICCT) program funded by DOE, Southern Company, and EPRI (Smith, L.L and Larsen, L.L., 1993) to evaluate NO_x control techniques in this unit. Overall, simulated properties were found to be in general agreement with measured properties for this set of firing conditions (Eddings, et al., 1997).

Figure 6-1 shows the predicted gas temperature distribution in the lower furnace simulation along several axial planes. Since the furnace is symmetrical about a vertical plane passing through the front and rear walls, only one-half of the furnace was modeled. The temperature distribution demonstrates how the fuel and air, which are fired from the front and back walls, mix and react in such a manner as to create a relatively hot plume of gases in the center of the furnace. These gases flow upward toward the nose and create a temperature distribution at the nose that can be characterized as being hottest in the region adjacent to the nose and decreasing in the direction of the front wall. Similarly, due to the firing configuration, the largest axial component of gas velocity is along the center of the furnace. This temperature and velocity distribution was seen to play a large role in determining the most effective upper furnace SNCR injection strategies.

6.1.2 Injection Strategies

The temperature measurements that were made in Hammond Unit 4 (Table 4-2), along with the results of the physical cold flow modeling work, served to provide a basis of the most promising injection scenarios to investigate in the CFD modeling effort. The physical cold flow modeling work for the geometry of Hammond Unit 4 indicated that high-energy

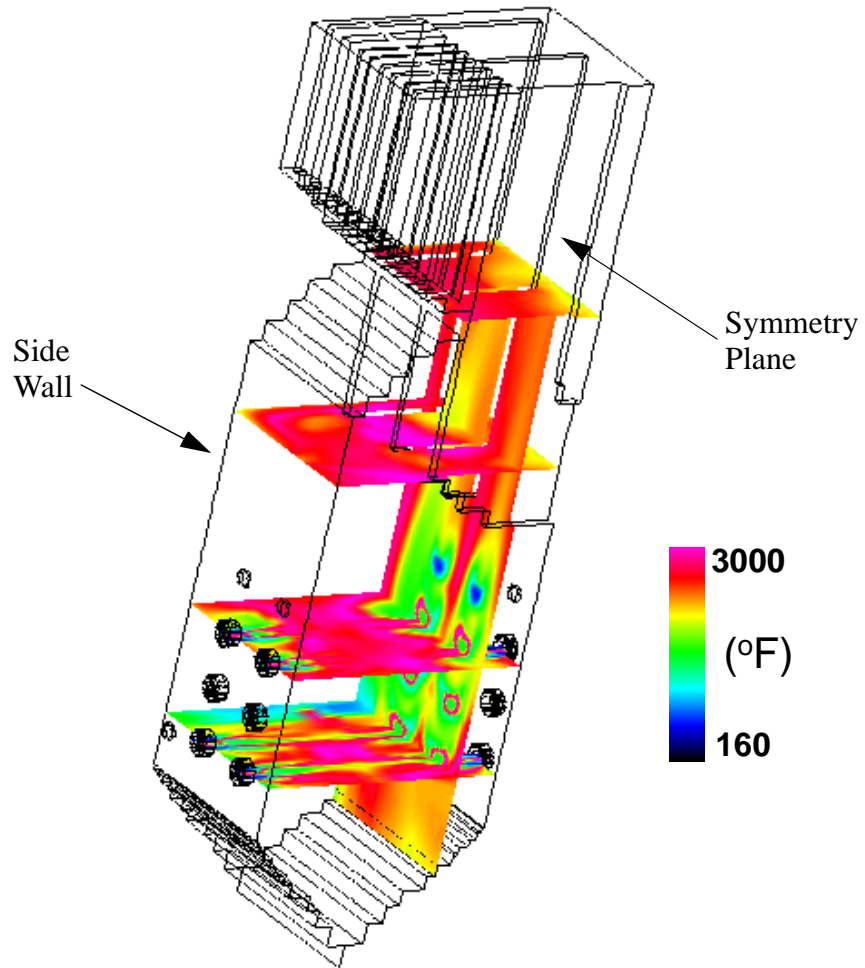


Figure 6-1: Predicted temperature distribution in the lower furnace of Hammond Unit 4.

injection, in general, achieved better mixing of reagent than low-energy injection. The five division panels extending from the front wall in the lower furnace up to the roof reduces the length scale of the largest turbulent eddies in the upper furnace to the distance between the panels. This reduction in the turbulence length scales tends to reduce the degree of advection of reagent away from the wall so that jet penetration into the furnace becomes more important. For a constant overall mass flowrate of injected reagent, the cold flow modeling indicated that the use of a single injector centered between the division panels achieved better mixing than did multiple injectors.

Guided by the results of that work, a number of injection scenarios were investigated using reacting flow CFD. Figure 6-2 shows schematically the injection locations that were examined in Hammond Unit 4. Front wall injection and lance injection at two different elevations above the tip of the nose were modeled. Both high-energy anhydrous ammonia and low-energy aqueous urea were considered. The high-energy anhydrous ammonia cases involved the use a significant quantity of carrier gas (0.2-1% of flue gas mass flow rate) to transport the reagent at high momentum. Air was used as the carrier gas for the model cases. A description of the eight cases that were modeled is given in Table 6-1.

Table 6-1: Summary of Injection Strategies for Hammond Unit 4

Strategy	# Injectors	Injector Locations, Orientation, and Reagent
1	NA	This case cannot be replicated in the field. Reagent uniformly mixed with flue gas at vertical plane at the tip of the nose. Anhydrous NH ₃ .
2	NA	This case cannot be replicated in the field. Reagent uniformly mixed at vertical plane one cavity downstream from the tip of the nose. Anhydrous NH ₃ .
3	6	Lance injectors centered between division panels 38 ft. directly above nose tip. Anhydrous NH ₃ . High-energy.
4	6	Lance injectors centered between division panels 6 ft. above nose tip, directed toward front wall. Anhydrous NH ₃ . High-energy.
5	20	Six wall injectors 14 ft. above nose, 14 lance injectors six ft. above nose tip, directed toward front wall. Anhydrous NH ₃ . High-energy.
6	6	Six wall injectors 14 ft. above nose. Anhydrous NH ₃ . High-energy.
7	20	Six wall injectors 14 ft. above nose, 14 lance injectors six feet directly above nose tip, directed toward roof. Anhydrous NH ₃ . High-energy.
8	22	20 front wall injectors at two elevations above the nose, 2 side wall injectors. Aqueous urea. Low-energy.

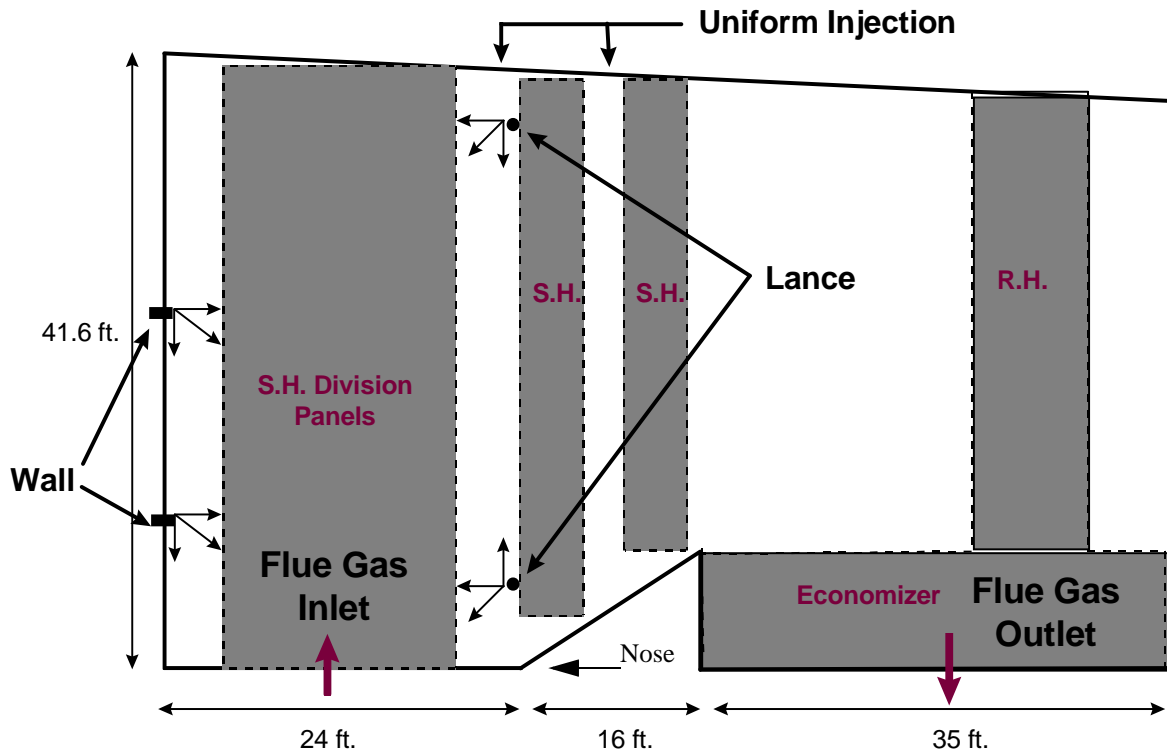


Figure 6-2: Schematic of Hammond Unit 4 upper furnace geometry indicating the injection strategies that were modeled.

6.1.3 Results

The CFD modeling study included examination of eight different injection strategies. Cases 1-7 considered anhydrous ammonia as the reagent, utilizing air as the carrier gas. Case 8 considered low-energy urea injection. A summary of the results of the simulations is given in Table 6-2. The table includes the normalized stoichiometric ratio (NSR), the average NO_x and NH₃ mole fractions, and the percent reduction of NO_x and peak NH₃ levels at the exit. The outlet plane where these values were determined is located 180° around from the inlet plane (Figure 6-2).

Figure 6-3 shows an isometric view of the lower furnace and upper furnace grid that were used in the simulations along with the interpolated inlet temperature. Using this inlet

Table 6-2: Predicted NO_x Reduction and NH₃ Slip for Hammond Unit 4, NO_{x,in}=310 ppm

Strategy	NSR	Avg. NO _x (ppm)	NO _x Reduction (%)	Avg. NH ₃ (ppm)	Max. NH ₃ (ppm)
1 (Fully-mixed Case)	1	213	31	<1	<1
2 (Fully-mixed Case)	1	172	45	<1	1
3 (Upper Lance Inj.)	1	211	32	74	1300
4 (Lower Lance Inj.)	1	299	4	<1	2
5 (Wall & Lance Inj.)	1	234	25	<1	7
6 (Front Wall Inj.)	1	222	29	3	45
6 (Front Wall Inj.)	2	206	34	10	140
7 (Wall & Lance Inj.)	1	229	26	1	18
7 (Wall & Lance Inj.)	2	212	32	4	75
8 (Low-energy Inj.)	1	215	31	31	336

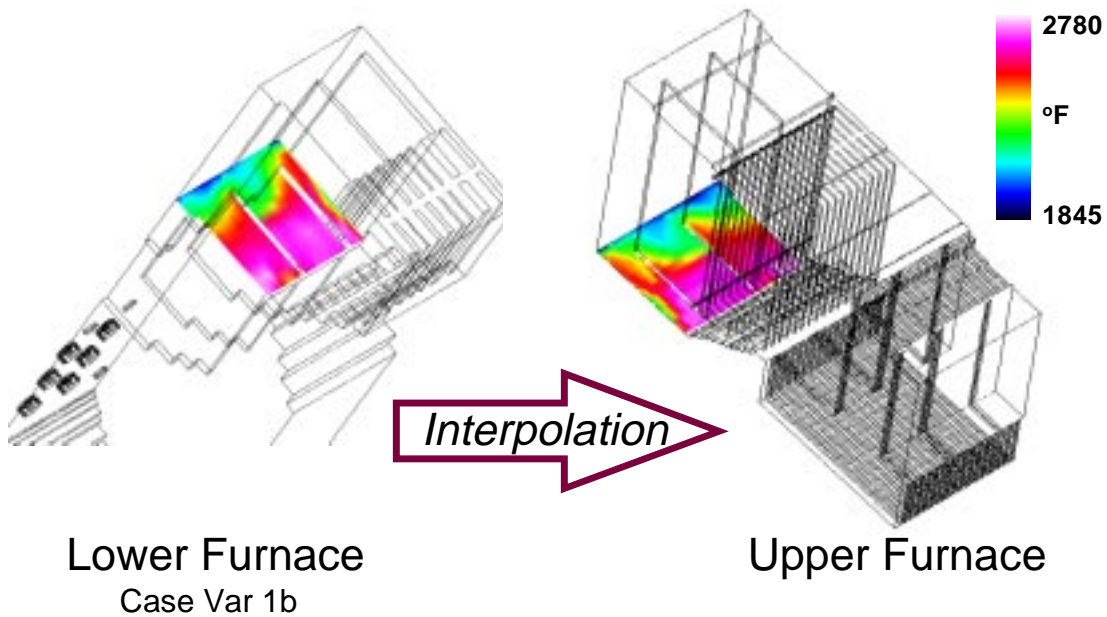


Figure 6-3: The inlet flue-gas temperature for the upper furnace geometry was obtained by interpolation from the lower furnace simulation.

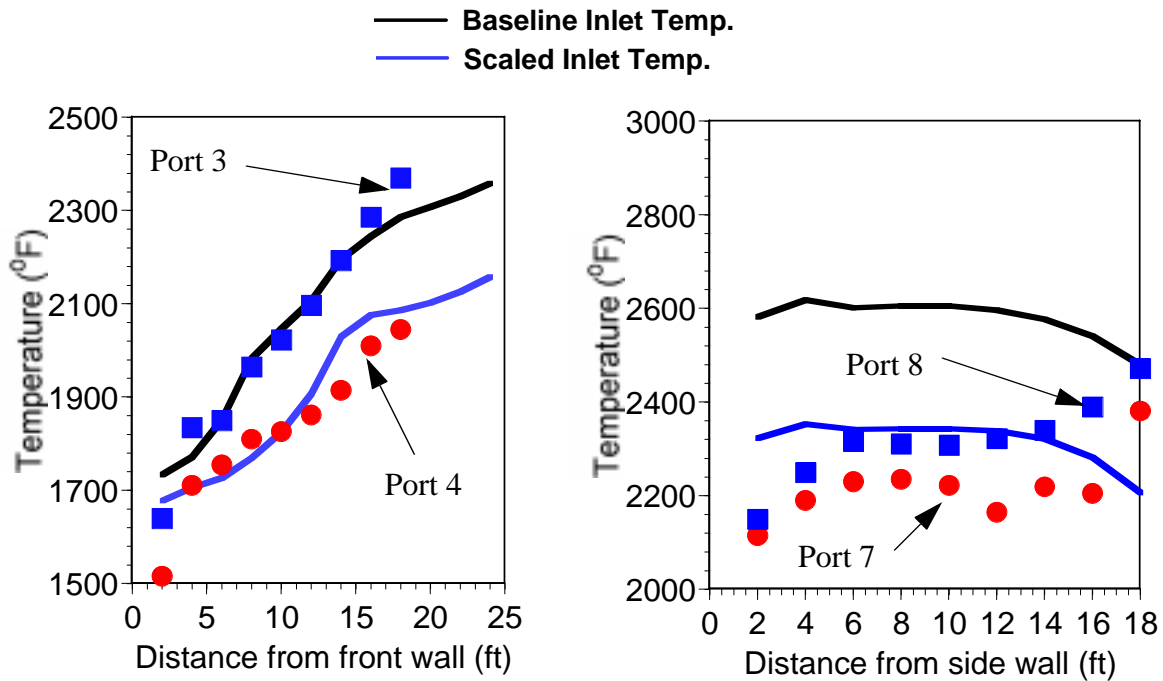


Figure 6-4: Comparison of measured temperatures in upper furnace of Hammond Unit 4 with scaled and unscaled predicted temperatures.

temperature distribution, comparison of the predicted and measured gas temperatures in the upper furnace showed some rather large differences in magnitude, most notably in the region immediately upstream of the convective passes above the nose. Figure 6-4 shows the comparison of the predicted and measured temperatures from several ports in the furnace (port locations are shown in Figure 4-2a). It was found that by scaling down the interpolated inlet temperature by 11% ($T_{\text{scaled}} = T_{\text{unscaled}} - 0.11(T_{\text{unscaled}} - 273.15)$), the measured and predicted temperatures were in better agreement (Figure 6-4). As a result, the interpolated inlet temperature was scaled in this manner for the cases discussed here. The predicted temperature distribution, reflecting the scaling at the inlet, is shown in Figure 6-5.

6.1.3.1 Convective Pass Injection (Fully-Mixed Cases)

The relatively high furnace exit gas temperatures in Hammond Unit 4 (Table 4-2) indicated that lance injection in the vicinity of the downstream convective passes may be necessary to achieve adequate reduction of NO_x. Cases 1-3 were considered to investigate the feasibility of convective cavity injection. Cases 1 and 2 represent conditions that cannot be replicated in practice. For those cases, it was assumed that NH₃ reagent was fully mixed with the flue gas and uniformly distributed throughout the vertical planes at the tip of the nose and one convective pass cavity downstream from the nose, respectively. The predictions from these

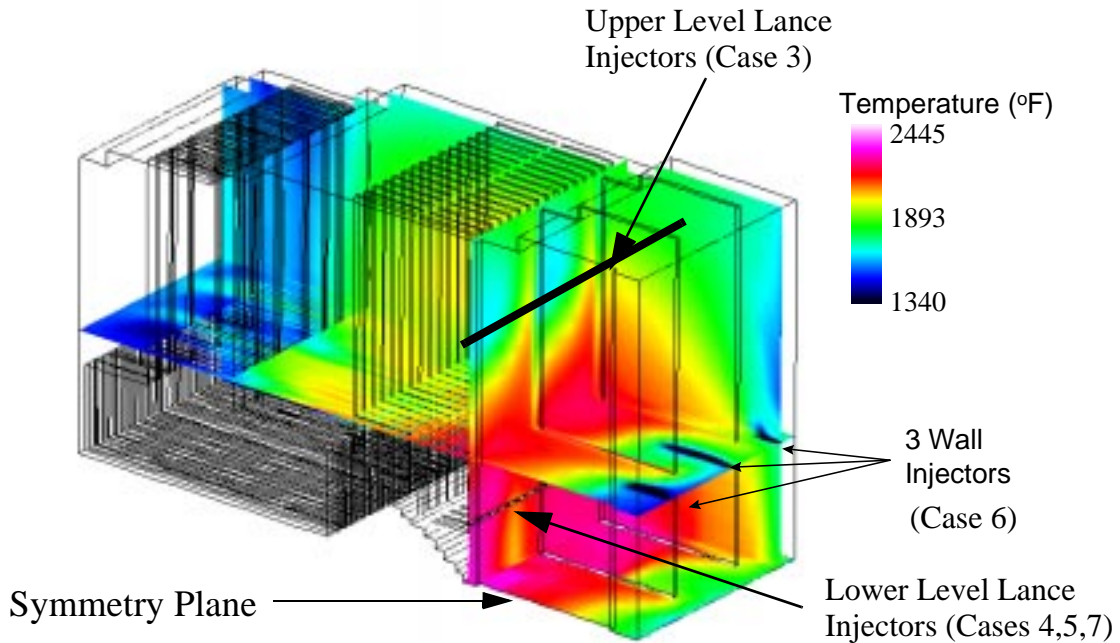


Figure 6-5: Predicted temperature distribution in the upper furnace of Hammond Unit 4. The particular case shown here involves injection of anhydrous ammonia from the front wall.

cases indicated that there is the potential to achieve relatively good reductions of NO_x (31% and 45%). These cases represent the NO_x reduction and ammonia slip that could be obtained if uniform mixing could be achieved in this region. Achieving this degree of mixing at these locations in practice is problematic since there is very limited residence time for mixing within the open space between the convective panels.

6.1.3.2 High-Energy Anhydrous Ammonia Injection

Case 3 indicates that if mixing is not complete, then NH₃ slip will be high. In this case, lance injectors were used to inject reagent just upstream of the first convective pass as shown in Figure 6-6. The injectors were angled downward 45° into the oncoming flue gas flow. Figure 6-5 shows that the predicted temperature distribution in the vicinity of these upper level injectors is on the order of 1800-1900°F, which is on the lower end of the SNCR temperature window. Figure 6-7 shows the predicted NO_x distribution for this case. Although NO_x reduction was quite good (32%), limited residence time for mixing coupled with cooler temperatures in the region of reagent injection contributed to high ammonia slip (74 ppm) in this case. In addition to the high average level of ammonia slip that was predicted in this case, the distribution of ammonia was seen to be highly variable. The ammonia slip at the exit plane could qualitatively be described as being high where the NO_x concentration was low, and vice versa. Localized levels of ammonia at the simulation exit were predicted to be as high as 1300

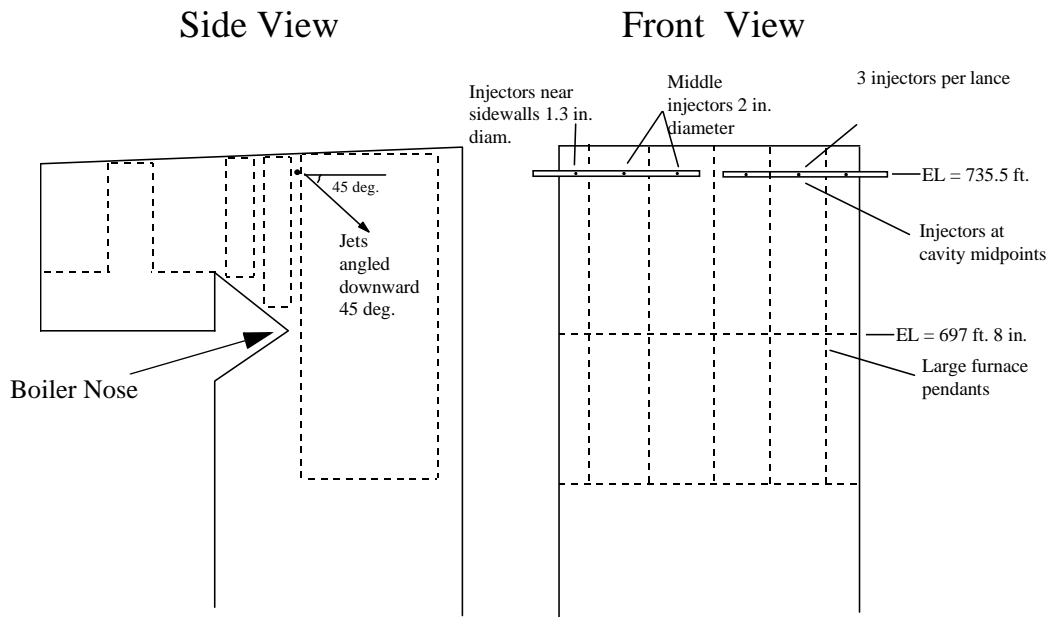


Figure 6-6: Schematic showing placement of injection nozzles for Hammond Case 3. A total of six nozzles on two injection lances are used.

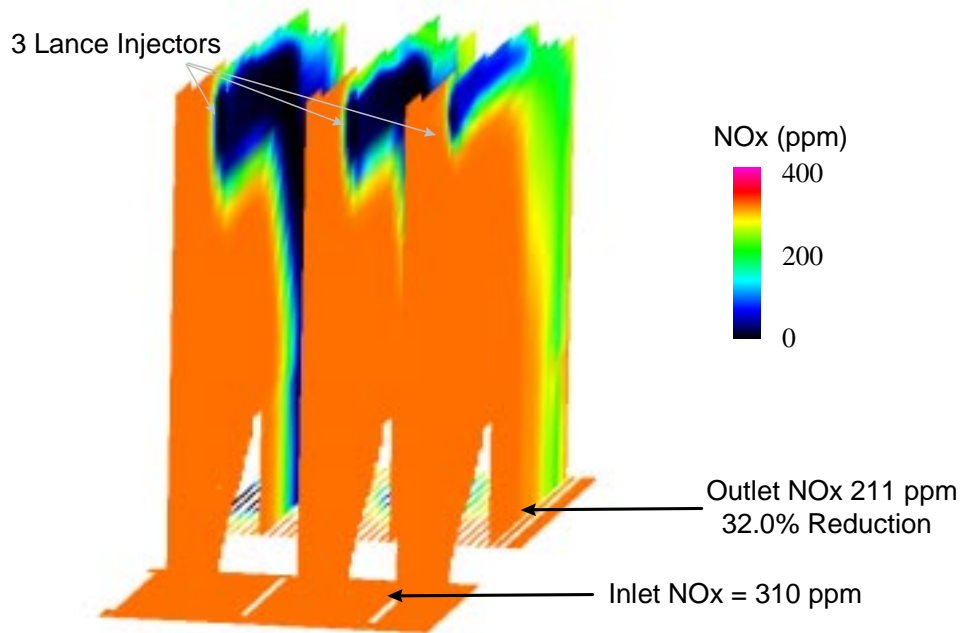


Figure 6-7: Predicted NOx distribution in Hammond Unit 4 for Case 3 involving upper level lance injection immediately upstream of the first convective pass.

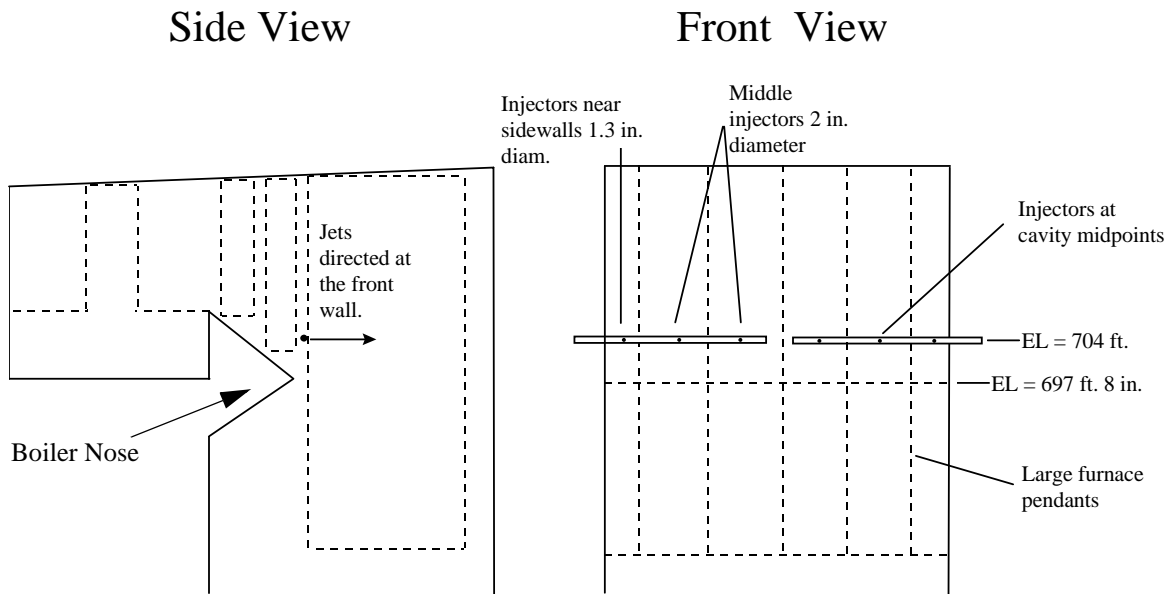


Figure 6-8: Schematic showing placement of nozzles in Hammond Unit 4 for Case 4. In this case, the lances are placed at a lower level, compared with Case 3, where the flue gas temperatures are higher.

ppm (Table 6-2). These observations are consistent with measured data in existing SNCR installations in utility boilers that involve injection of SNCR reagent only in the vicinity of the convective passes (Lin, 1992; Shore, 1993).

Cases 4-8 involve strategies utilizing furnace injection further upstream of the convective passes. Case 4 involved lance injection similar to that utilized in Case 3, but at a lower elevation (Figure 6-8). In this case, six lance-based injectors, each centered in the gap between the five division panels, were directed toward the front wall. The predicted temperature distribution in the vicinity of these injectors (Figure 6-5) shows that the gas temperature there is on the order of 2100-2300°F, which is in the upper limit of the SNCR temperature window. The effect of the increased flue gas temperature on the predicted NO_x reduction is shown in Figure 6-9. The net NO_x reduction drops to 4% for this case with 0 ppm NH₃ slip.

Case 5 involved the use of front wall injectors in conjunction with lower level lance injectors (Figure 6-10). From a mixing standpoint, this injection strategy was seen to be the best approach tested in the physical cold flow modeling work (Martz & Muzio, 1997). In this case, there were 14 injectors in the lances above the nose at a 45° angle to the horizontal, as shown, and 6 wall injectors at a 22.5° angle to the horizontal. Figure 6-5 shows that the gas temperature in the vicinity of the wall injectors is more optimal for SNCR than for the lance injectors. NO_x reduction for this case was much improved (25%) over that seen in Case 4 due to the addition of the wall injectors. Very little NO_x reduction was achieved from the lower

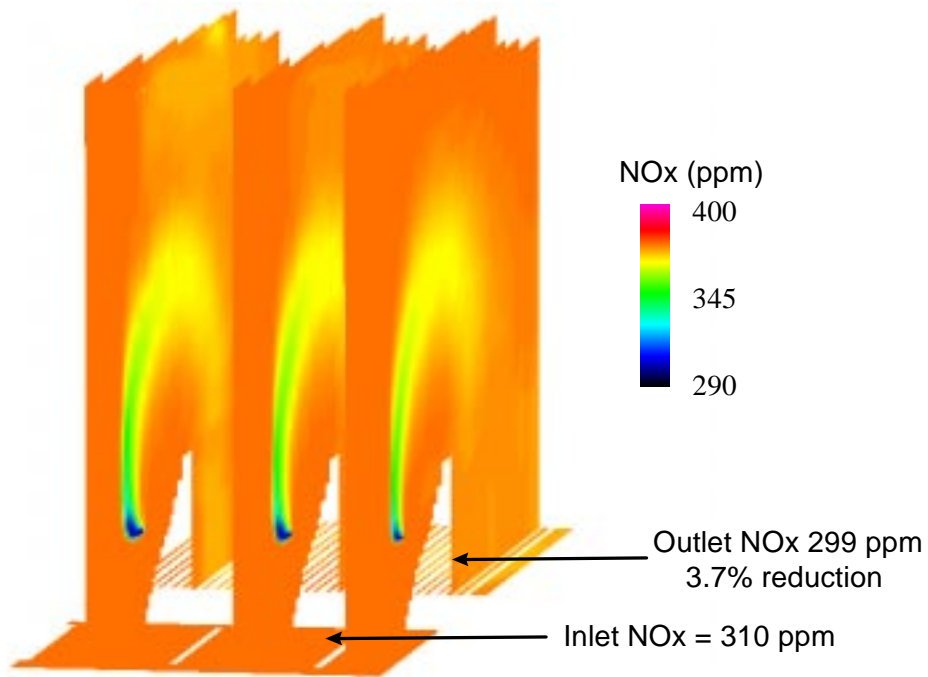


Figure 6-9: Predicted NOx distribution in Hammond Unit 4 for Case 4 involving lower level lance injection of anhydrous ammonia. This strategy results in almost no net decrease in NOx.

level lance injectors due to the high flue gas temperatures there, consistent with the results of Case 4.

Although the injection strategy in Case 5 was optimum from a mixing standpoint, the reagent injected down into the oncoming flue gas from the lower level lances achieved very little overall NOx reduction. Most of the NOx removal was due to the wall injectors. In Case 6, only wall injectors located 14 feet above the tip of the nose were utilized (Figure 6-11). Figure 6-12 shows the predicted mixture fraction and NOx distributions for this case. The mixture fraction is the mass fraction of injected reagent and carrier gas at each location. It is a measure of the degree of mixing between the reagent and the flue gas. Figure 6-12a shows that by utilizing only front wall injectors, the flue gas in the lower region of the furnace is left untreated. Since the temperature of the flue gas in this region is more optimal for SNCR and front wall injection provides additional residence time for mixing and chemical reaction, NOx reduction is good (29%) with low average ammonia slip (3 ppm). When the NSR is increased from one to two, the predicted NOx reduction increases slightly (34%) with a corresponding increase in ammonia slip (10 ppm).

Case 7 (Figure 6-13) is a slight variation on Case 5. Overall mixing is quite poor in Case 6 since the lower level flue gases are left untreated. Overall mixing was much better in Case 5 because of the lower level lance injectors. However, in Case 5, the reagent injected from the lances provided little benefit to removing NO_x because of the high gas temperature in the region below the lance. The reagent was directed down into the oncoming hot flue gas flow which increased the residence time in this hot region. In Case 7, the nozzles were directed toward the roof to reduce the residence time in this hot region and decrease the amount of ammonia that would be oxidized to form additional NO_x. Figure 6-14 shows the predicted mixture fraction and NO_x reduction for this case. Comparison of Figures 6-12a and 6-14a shows that mixing of the reagent with the flue gas is better in Case 7 than in Case 6. However, the overall NO_x reduction is slightly less (26%) with a comparable drop in ammonia slip (1 ppm). Consistent with the predictions for Case 6, increasing the NSR from one to two provides only a small increase in NO_x reduction (32%) with a small increase in ammonia slip (4 ppm). This case implied that regardless of how the injectors from the lower level lances are oriented, they provide little or no benefit to overall NO_x reduction because of the high gas temperature. At reduced load, however, when gas temperatures are lower, there would probably be a benefit to placing injection lances at this lower elevation.

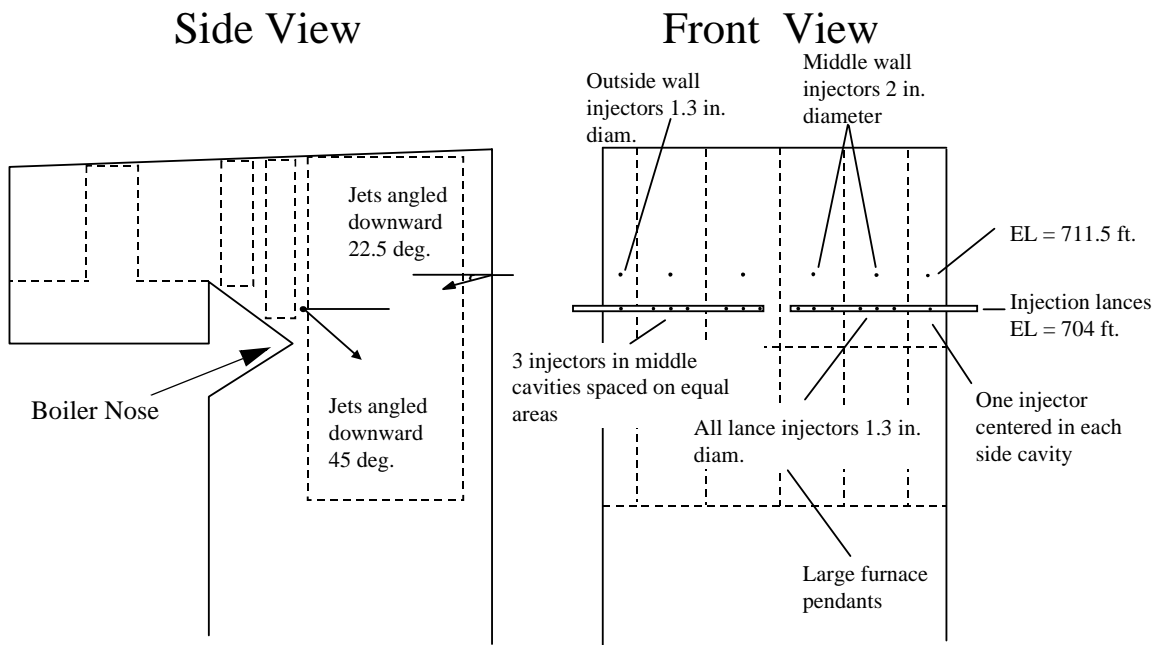


Figure 6-10: Injection strategy for Hammond Case 5. This injection strategy was very good from a mixing standpoint.

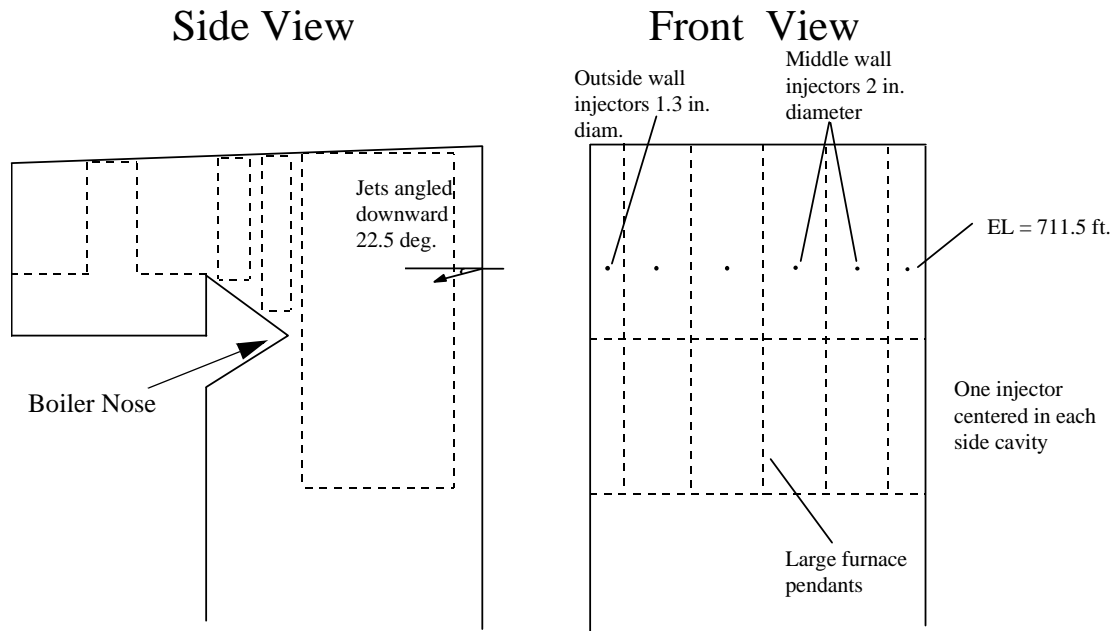


Figure 6-11: Schematic showing placement of nozzles in Hammond Case 6. This strategy is the same as that used for Case 5 without the injection lances.

6.1.3.3 Low-Energy Aqueous Urea Injection

Case 8 involved the use of low-energy aqueous urea injection. In this modeled case, a total of 20 injectors were placed at two elevations on the front wall, and one additional injector was placed on each side wall for a total of 22 injectors as shown in Figure 6-15. The injected droplets were considered to consist of a 10% solution of urea in water and the droplet size distribution was assumed to have a Sauter mean diameter of 100 μm . A 30° full cone spray angle was modeled for each injector and the droplets were given a specified initial velocity of 15 m/s. The particle chemistry was modeled by a two step process: 1) water evaporation and 2) solid urea thermal decomposition. No urea was allowed to decompose prior to 100% water evaporation. The rates associated with the thermal decomposition of the urea are fast so that after the water evaporates, the urea particle heats up rather quickly and decomposes into equal parts of gaseous ammonia (NH_3) and isocyanic acid (HNCO) which subsequently react in the gas phase.

This low momentum associated with the injected reagent in this case is in contrast to the high momentum of the injected reagent in the others. The effect of this on penetration of the reagent into the furnace is shown in Figure 6-16. This figure shows that a typical urea droplet (107 μm) from Case 8 has very limited penetration into the furnace compared with the high-

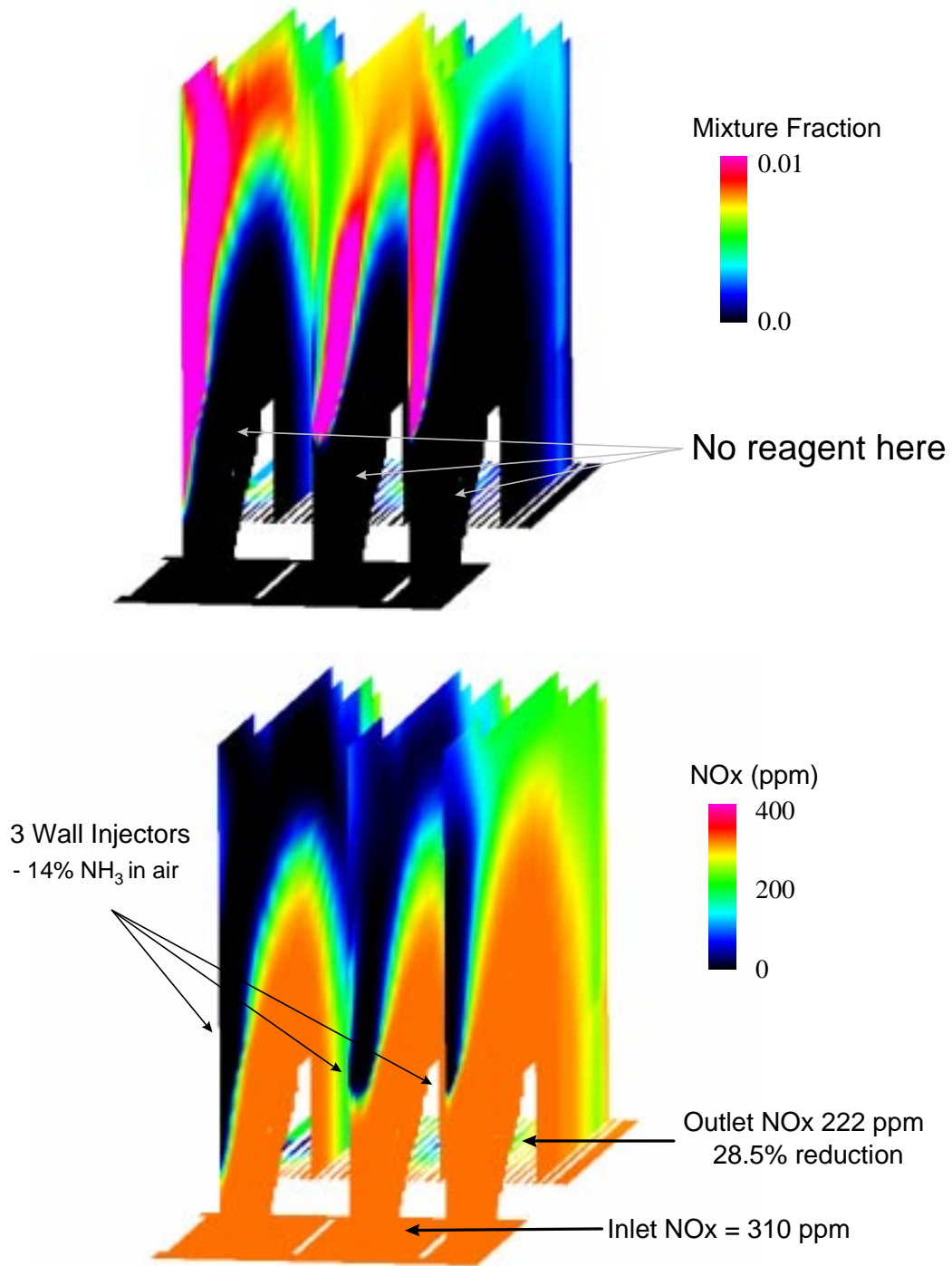


Figure 6-12: Predicted mixture fraction and NO_x distribution for Hammond Case 6. a) The mixture fraction represents the mass fraction of injected reagent and carrier gas at each point, so is a measure of the degree of mixing. b) Predicted NO_x distribution.

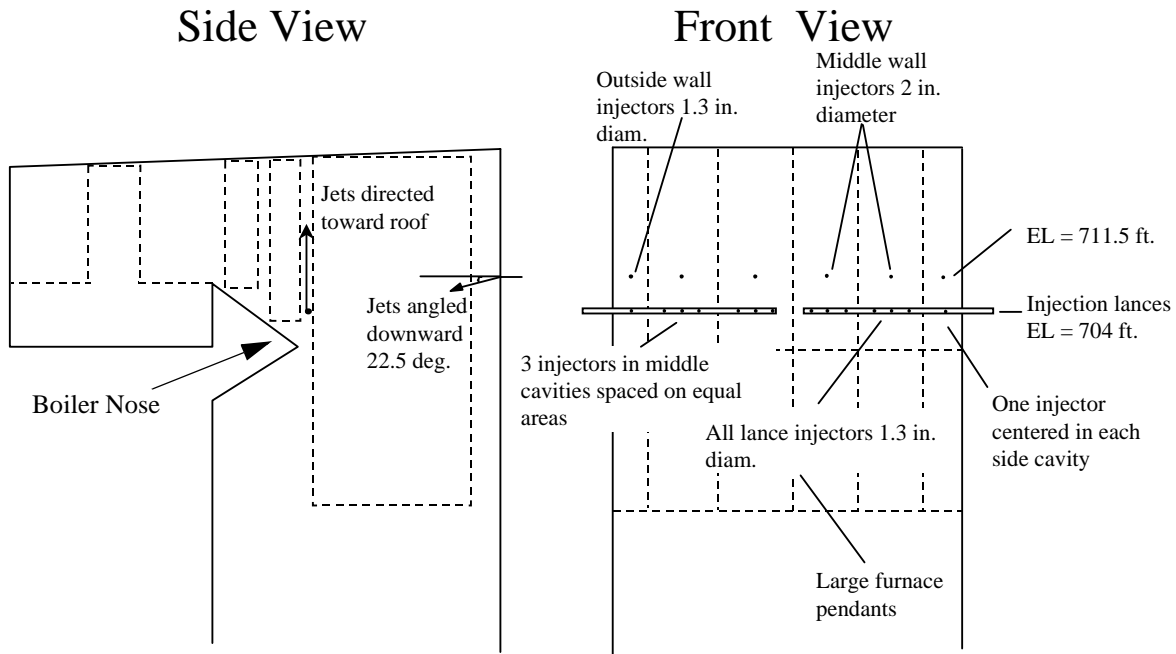


Figure 6-13: Schematic showing placement of injectors for Hammond Case 7. This case is similar to Case 5, the difference being that in this case, the lance injectors are directed toward the roof.

energy jet from Case 6. The effect of this on the overall distribution of reagent into the furnace is illustrated in Figure 6-17. In the low-energy urea case (Case 8), much of the reagent concentrates near the center of the furnace in comparison to the high-energy ammonia case (Case 6). This is a result of the lack of penetration of the reagent into the furnace. In Case 8, much of the reagent from the injectors adjacent to the side wall is convected upward and away from the side wall by the flue gas. Since there is roughly a 1 meter gap between the front wall and the edge of the wing walls, some of this reagent slips through this gap over into the adjacent cavity where it is then channeled between the wing walls and downstream convective panels. So, as is seen in Figure 6-17, the injected reagent is more evenly distributed throughout the furnace in Case 6 than in Case 8.

Figure 6-18 shows the predicted NO_x reduction for Case 8. In comparison with Case 6, the net NO_x reduction is slightly higher (31%), but the average ammonia slip is also significantly higher (31 ppm) for NSR=1. The higher ammonia slip is a result of the poor distribution of reagent. Although the average ammonia slip is 31 ppm, peak ammonia levels at the exit were predicted to be as high as 330 ppm.

6.1.3.4 Spatially Dependent Inlet NO_x Distribution

In each of Cases 1-8, a uniform distribution of NO_x (310 ppm) was imposed at the inlet to the upper furnace. The simulations of the lower furnace, however, indicated that NO_x distribution

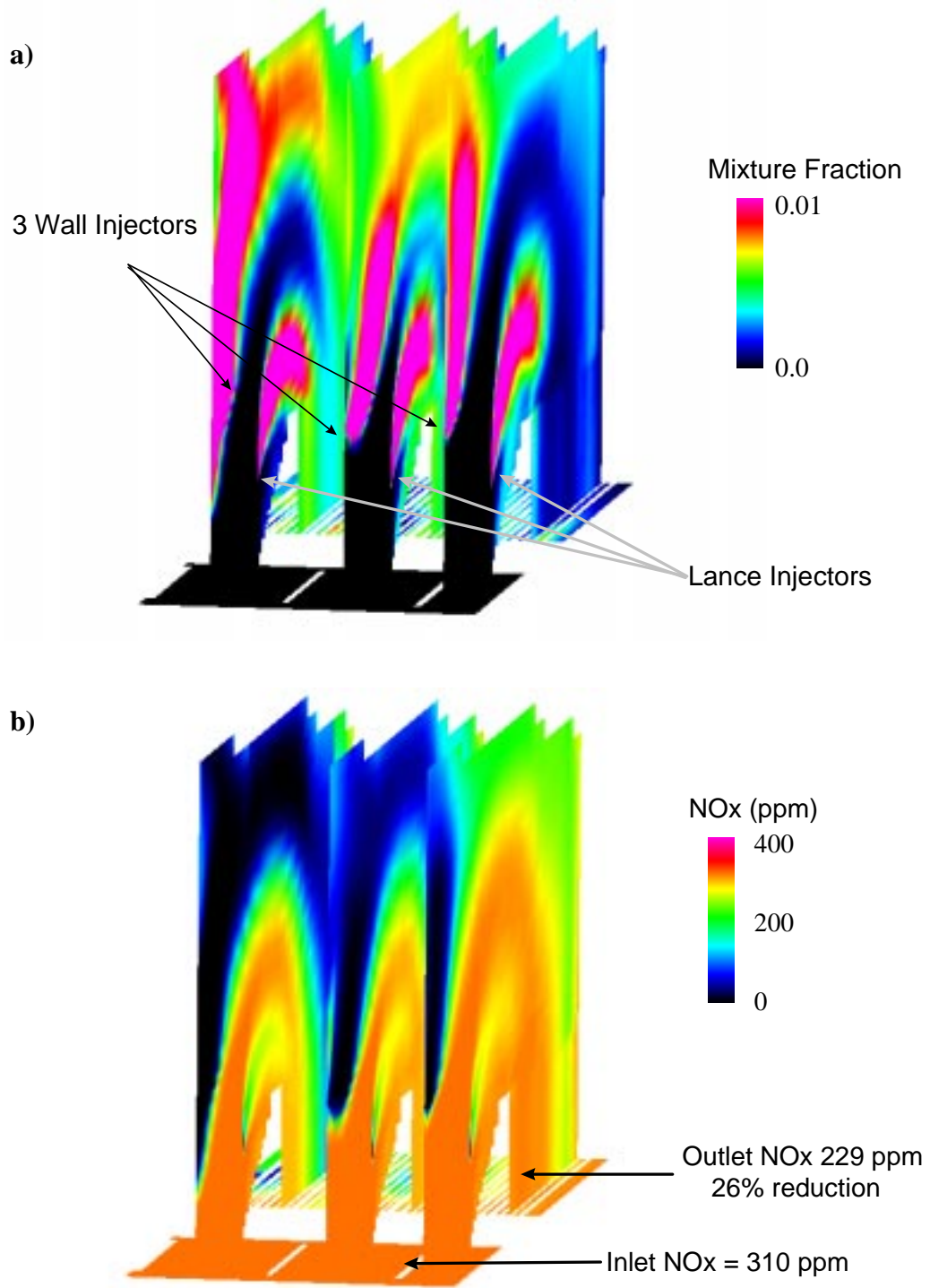


Figure 6-14: Predicted mixture fraction and NOx distribution for Hammond Case 7. Overall reagent mixing is much better for this case than for Case 6, but overall NOx reduction is slightly less.

at the nose is very nonuniform. To determine the effect of this expected nonuniform distribution on the upper furnace NO_x reduction, an additional case was completed to impose the predicted NO_x distribution at the nose in the upper furnace simulation for Case 6. The results of this study showed very little difference, in the predicted NO_x reduction (30%) and NH₃ slip (3 ppm), with the results obtained assuming a uniform inlet NO_x distribution (NO_x 29%; NH₃ slip 3 ppm). The predicted NO_x distribution for this case is shown in Figure 6-19.

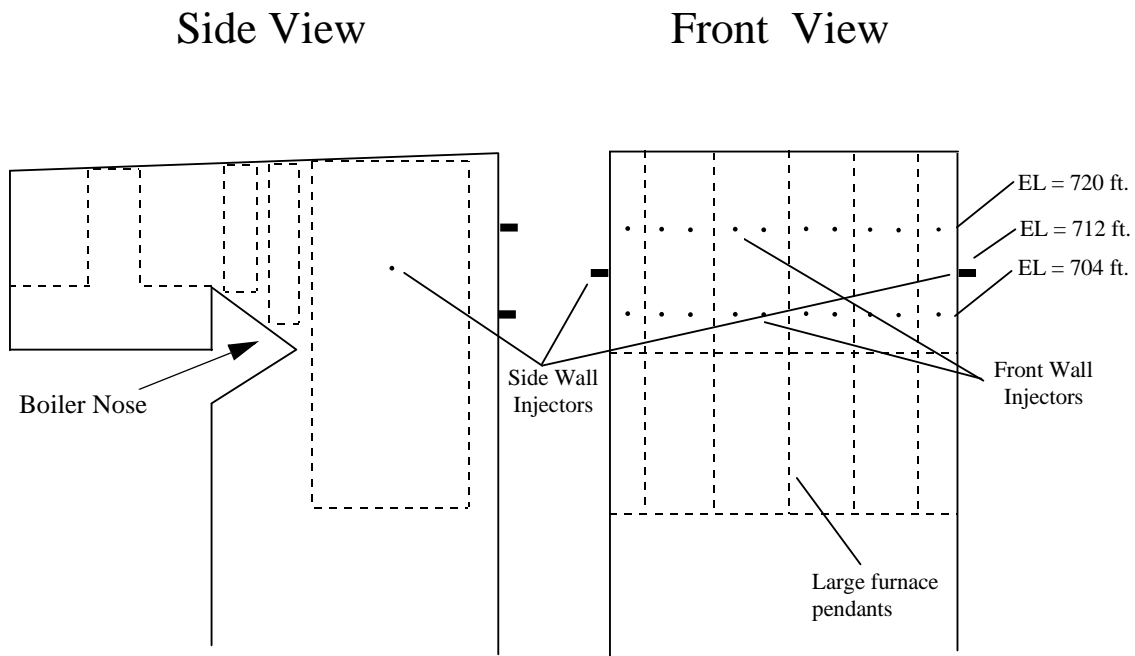
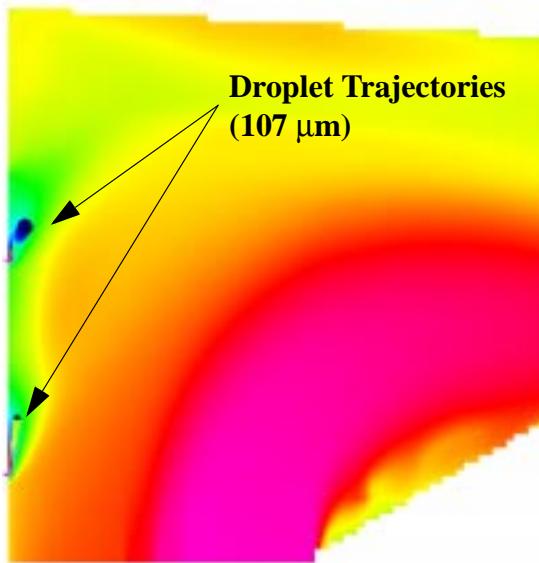


Figure 6-15: Schematic Case 8 injection strategy for Hammond Unit 4. This strategy involves the use of 22 low-energy aqueous urea injectors.

a) Case 8



b) Case 6

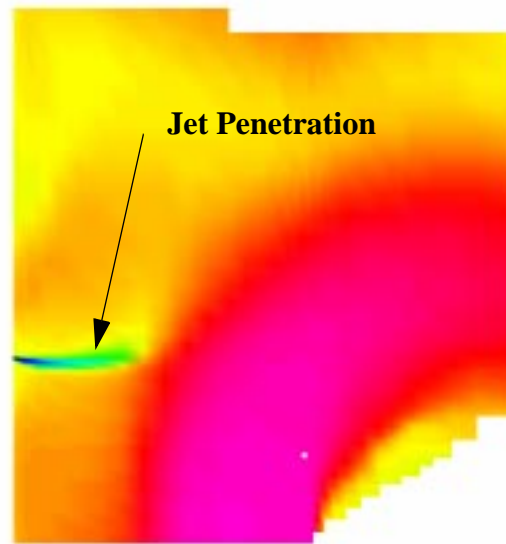


Figure 6-16: Comparison of jet penetration in Case 6 (high-energy anhydrous ammonia) and Case 8 (low-energy aqueous urea) in terms of gas temperature. a) Case 8. The mean trajectories of 107 μm droplets are shown here. The trajectories are colored by urea mass fraction in the droplet. b) Case 6. The penetration of the high-energy jet in this case exceeds that of the droplets in the low-energy urea case.

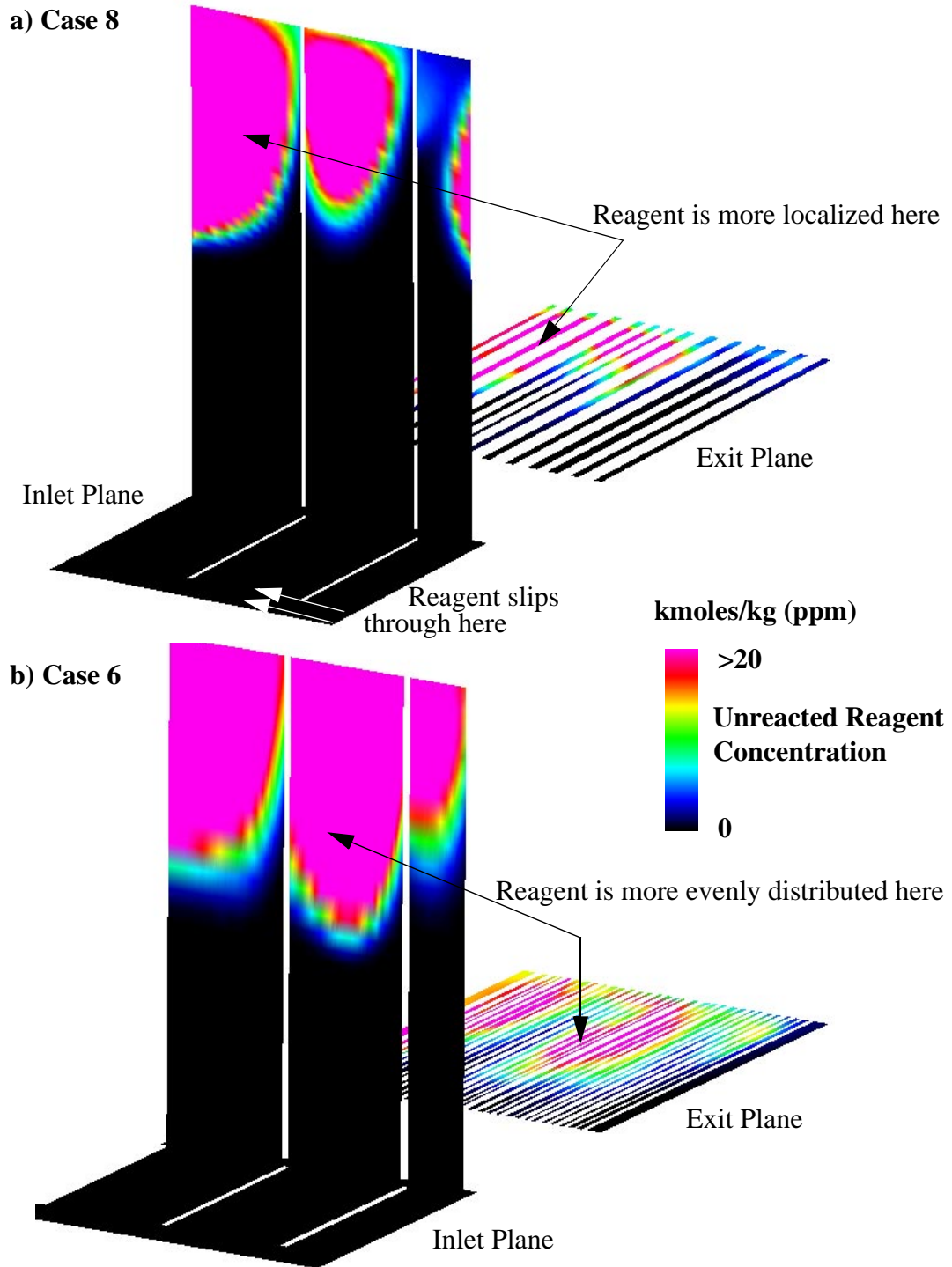


Figure 6-17: Comparison of reagent distribution between Case 8 and Case 6 assuming no chemical reaction with the flue gas. Reagent dispersion is better in Case 6 (high-energy) than in Case 8 (low-energy) even though more injectors are used in Case 8.

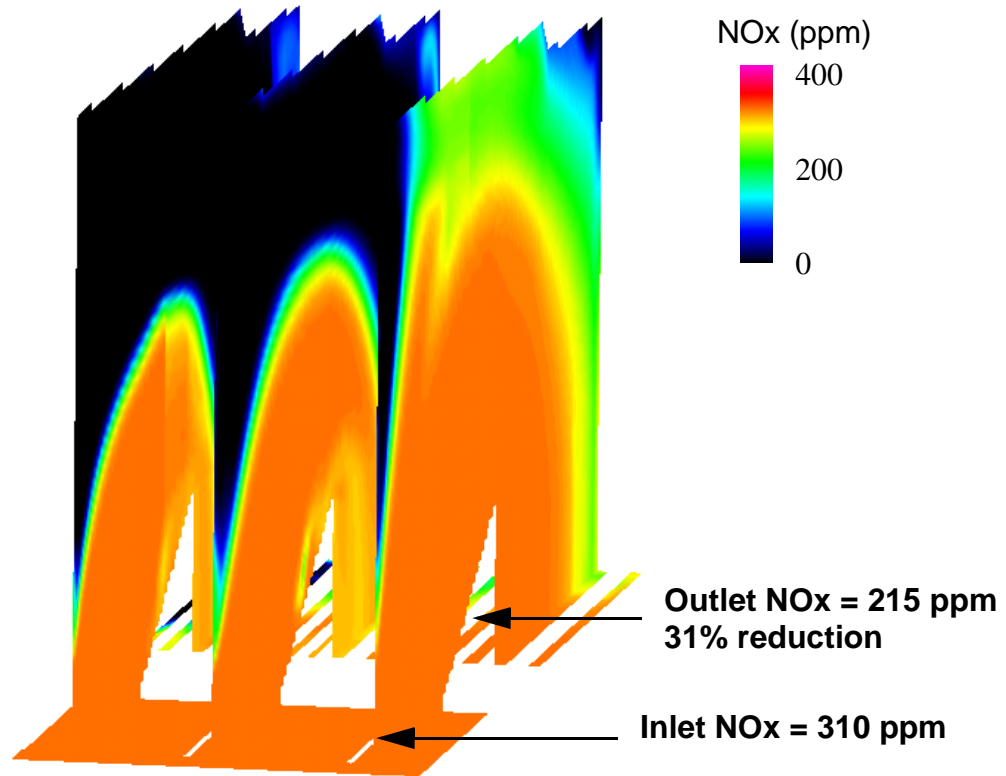


Figure 6-18: Predicted NOx distribution for Hammond Case 8 involving the use of low-energy aqueous urea injectors.

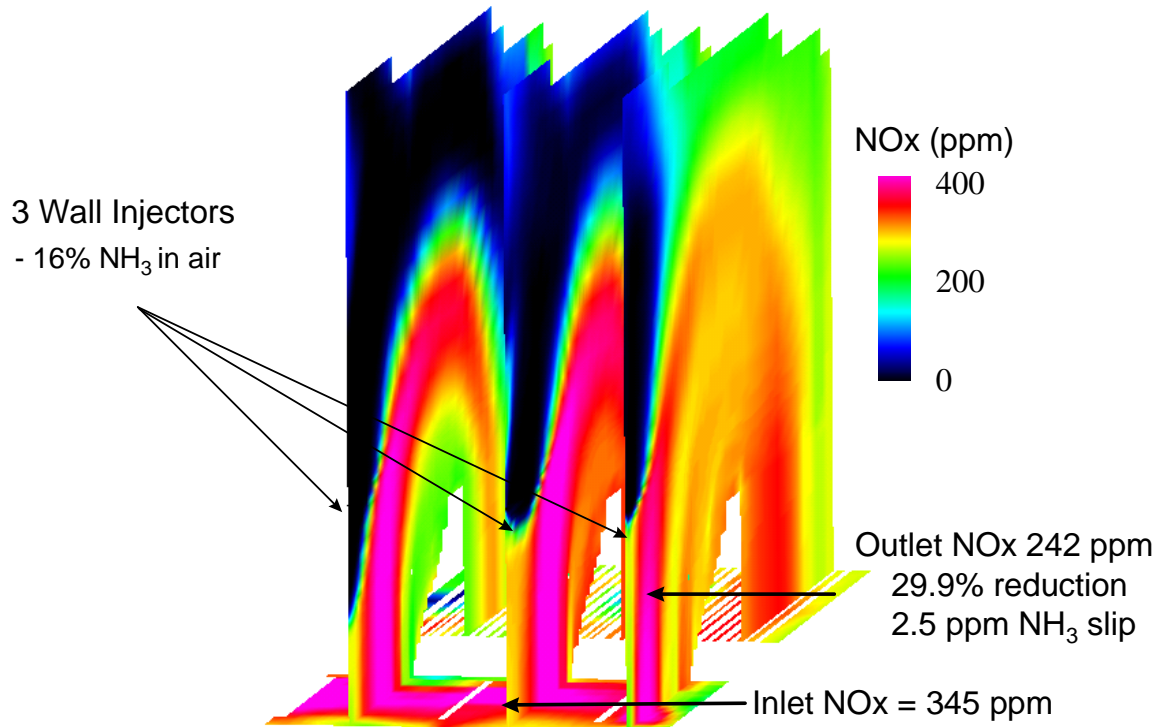


Figure 6-19: Predicted NOx distribution in Hammond Case 6 assuming a nonuniform inlet distribution at the furnace nose. The NOx distribution used here was interpolated from the results of the simulation of the lower furnace of Hammond Unit 4.

6.1.3.5 Summary of Hammond Unit 4 Predictions

The results of the Hammond simulations indicate that NO_x reductions of 30-35 percent with less than 5 ppm ammonia slip appear feasible during steady state boiler operations at full load. Furnace operating factors such as unit load, fuel type, soot-blowing cycles, operating profile, and mill patterns are expected to impact these predictions. Doubling the NSR from one to two appears to result in relatively small increases in NO_x reduction (~5%). Ammonia slip is predicted to have high spatial variability with peak levels an order of magnitude higher than the average. Although limited to a small region of the total exit area, the impact of concentrated regions of ammonia slip could result in localized pluggage of an annular region of the air heater as it rotates through the high slip zone. In practice, however, reagent flowrates to individual injectors could be biased in an attempt to minimize locally high ammonia slip concentrations.

6.2 Wansley Unit 1

Wansley Unit 1 utilizes a twin-furnace, tangentially fired 880 MW supercritical Combustion Engineering boiler that has been retrofitted with ABB C-E Services' Low-NO_x Concentric Firing System Level 2. The entire furnace cross-section measures nominally 96 feet wide and 43 feet deep. The unit is designed to provide 6.2×10^6 pounds of steam per hour at a pressure of 3500 psig. Superheat and reheat steam temperatures are 1000°F. It has a balanced draft design with two Ljungstrom air preheaters. Particulate emissions are controlled by a cold side electrostatic precipitator. This unit is typical of other large T-fired boilers of its vintage (supercritical boilers built in the late 60s or early 70s that have been retrofitted with a low-NO_x firing system to comply with Clean Air legislation).

6.2.1 Lower Furnace Simulation

Since this unit is a twin furnace that is nominally symmetric about the center waterwall, only the right hand (RH) furnace was modeled. Inlet properties were assumed to be characteristic of full load "normal" conditions while firing the Kerr McGee coal. Actual control room data were used to specify input information for fuel and air flow rates and inlet temperatures so that simulated properties could be compared with measurements taken under the same steady state conditions.

Figure 6-20 shows the predicted temperature variation in the lower furnace. The tangential firing pattern creates peak temperatures near the center of the "firing circle". This distribution was similarly observed in the temperature measurements that were taken in the furnace. The

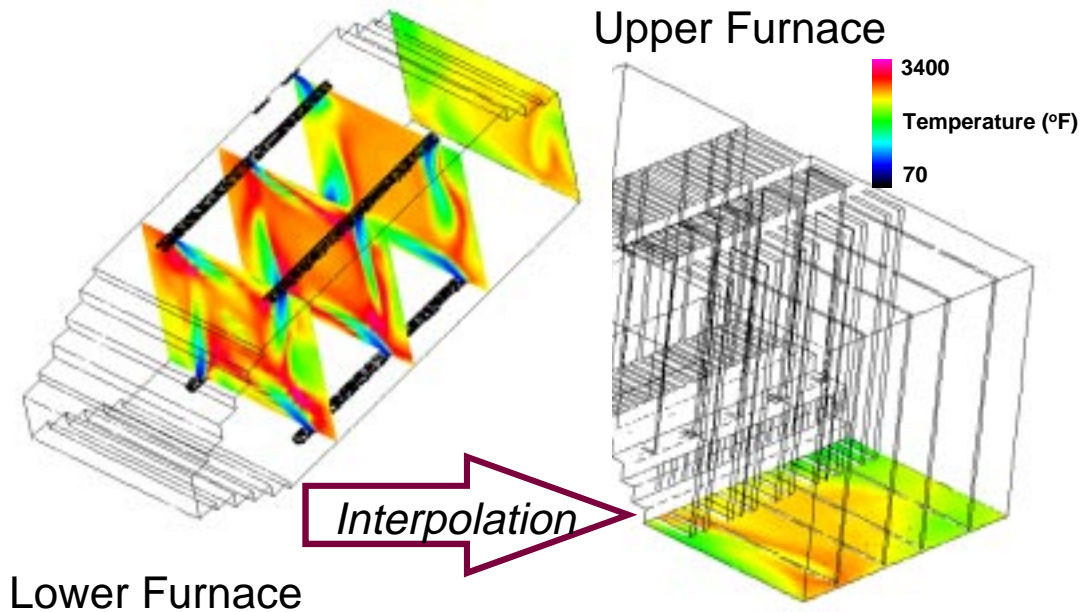


Figure 6-20: Computed lower furnace temperature distribution for Wansley Unit 1. Properties at the nose of the lower furnace simulation are interpolated onto the upper furnace grid for the SNCR simulations. The tangential firing geometry results in peak temperatures in the center of the firing circle.

simulated temperatures were in general agreement with the measurements taken near the furnace exit and in the downstream convective passes (Table 4-1). Figure 6-21 shows the computed and interpolated temperature and axial velocity distribution at the horizontal plane at the nose.

6.2.2 Injection Strategies

The high furnace exit gas temperatures (approximately 2400°F) that were both measured and predicted at the exit of Wansley Unit 1 made the feasibility of achieving significant NO_x reduction using SNCR questionable at the outset of this study. The furnace exit gas temperatures are well above the temperature range for aqueous urea (1850°F to 2100°F) and ammonia. Temperatures in the downstream convective passes (Table 4-1) are more optimal but short residence times coupled with difficulty in achieving uniform mixing in the convective passes can make injection in these regions problematic. Figure 6-22 shows the comparison between measured and predicted upper furnace temperatures in Wansley Unit 1 near the convective passes indicating good agreement between the two.

The temperature measurements and the results of the physical cold flow modeling, coupled with the practical equipment and maintenance constraints concerning placement of injectors,

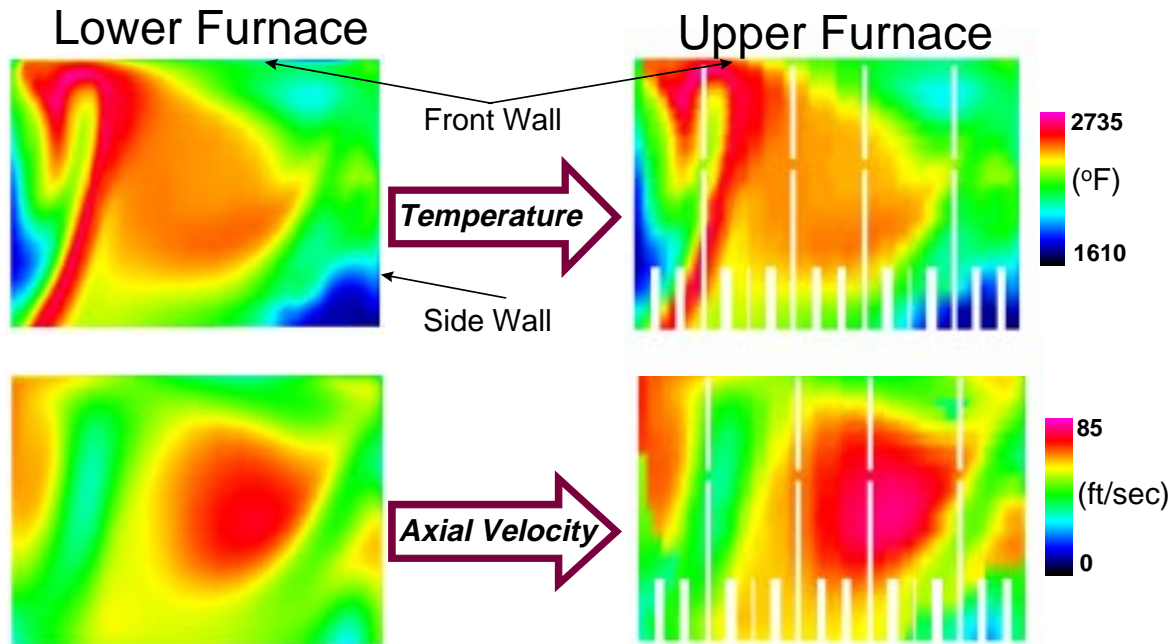


Figure 6-21: Comparison between computed lower furnace properties with interpolated properties at the inlet to the upper furnace for the simulation of Wansley Unit 1. The interpolation plane is the horizontal plane at the furnace nose. Computed and interpolated temperature and axial velocity are shown here.

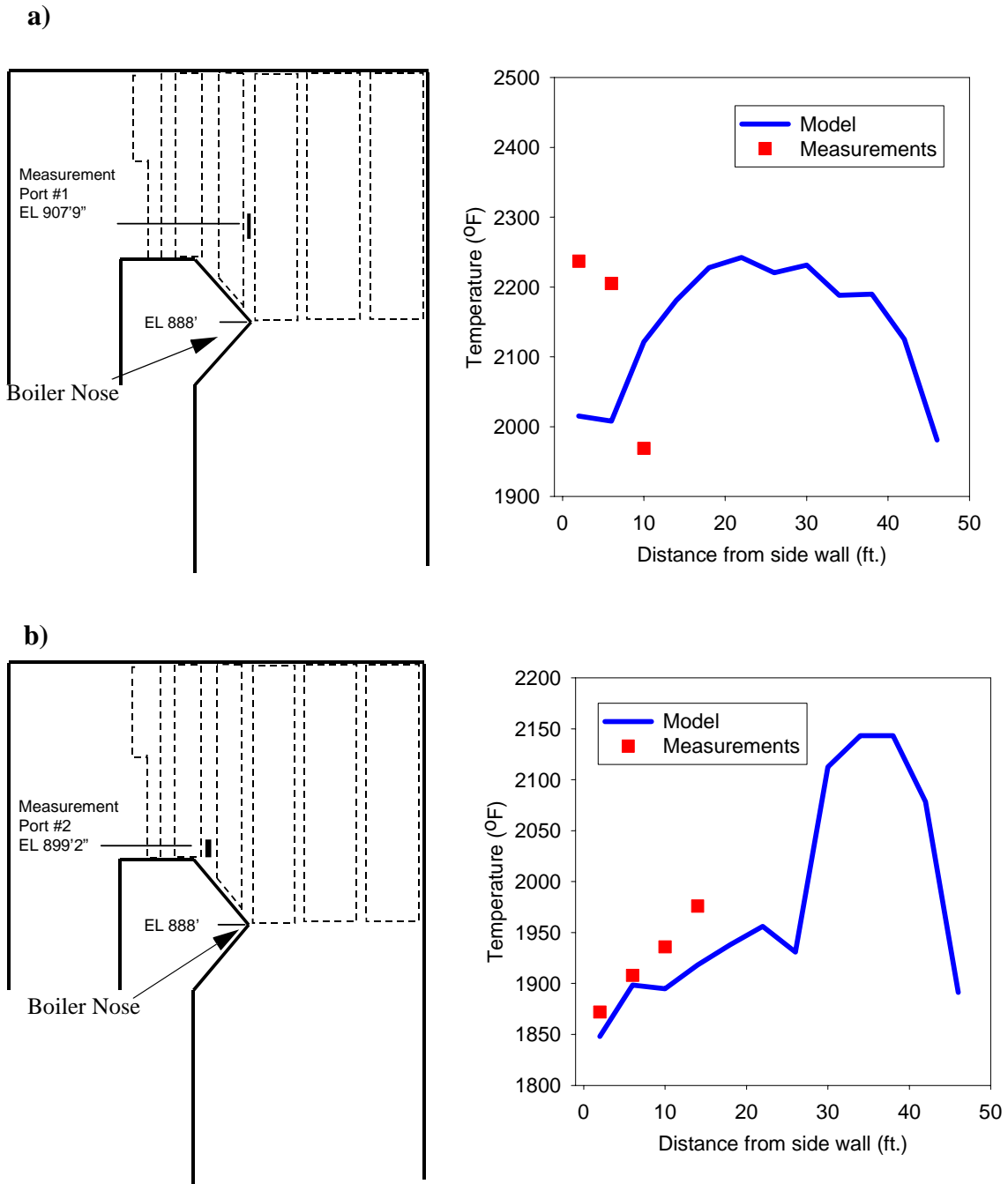


Figure 6-22: Comparison between measured and predicted gas temperatures in Wansley Unit 1. a) Comparisons at port 1 located directly above the nose tip. b) Comparisons at port 2 located one cavity downstream from the nose.

Table 6-3: Summary of Injection Strategies for Wansley Unit 1

Strategy	# Injectors	Injector Locations, Orientation, and Reagent
1	NA	Reagent uniformly mixed with flue gas at vertical plane at the tip of the nose. Anhydrous NH ₃ .
2	NA	Reagent uniformly mixed with flue gas at vertical plane one cavity downstream of nose. Anhydrous NH ₃ .
3	10	Five floor injectors at tip of nose pointing toward roof, five roof injectors pointing toward floor. Anhydrous NH ₃ . High-energy.
4	5	Wall injectors centered between division panels 5 ft. above nose tip. Anhydrous NH ₃ . High-energy.
5	10	Five wall injectors 29 ft. above nose, five lance injectors extending 12 ft. from front wall, five ft. above nose tip. Anhydrous NH ₃ . High-energy.
6	5	Wall injectors centered between division panels, 29 ft. above nose. Aqueous urea. High-energy.
7	22	20 front wall injectors at two elevations above the nose, two side wall injectors. Aqueous urea. Low-energy.

led to the matrix of injection scenarios shown in Table 6-3 and Figure 6-23. For Wansley Unit 1, seven injection strategies were modeled: five involving high-energy anhydrous ammonia, one involving high-energy aqueous urea, and one involving low-energy aqueous urea. Both wall and lance injection strategies were considered. The high-energy cases involved the use of a large quantity of carrier air (0.5 - 1% of flue gas mass flow rate) to achieve high jet momentum for transporting the reagent. Of the five injection strategies utilizing anhydrous ammonia, three included reagent injection in the convective passes where flue gas temperatures quickly drop through the optimum SNCR temperature range. The other two anhydrous ammonia cases involved a combination of front wall and lance injection. The high-energy aqueous ammonia case utilized upper level front wall injectors centered between the four division panels. The low-energy aqueous urea case utilized more than double the number of injectors placed on both the front and side walls. In both, the droplets were considered to be a 10% solution of urea in water, with a Sauter Mean Diameter (SMD) of 100 μm .

6.2.3 Results

The results of the simulations, showing the predicted average outlet NO_x and NH₃ mole fractions (in ppm) as well as the predicted NO_x reduction (%) and peak ammonia slip, are shown in Table 6-4. All results are for furnace operation at full load. As expected, NO_x removals were lower than those predicted for Hammond Unit 4. The high furnace exit gas temperatures led to prediction of increased NH₃ oxidation in these hot zones, contributing to reduced overall NO_x reduction. Figure 6-24 shows the predicted upper furnace temperature distribution, computed for Case 4, showing the extremely high furnace exit temperatures.

Uniform Injection (Fully-Mixed Cases)

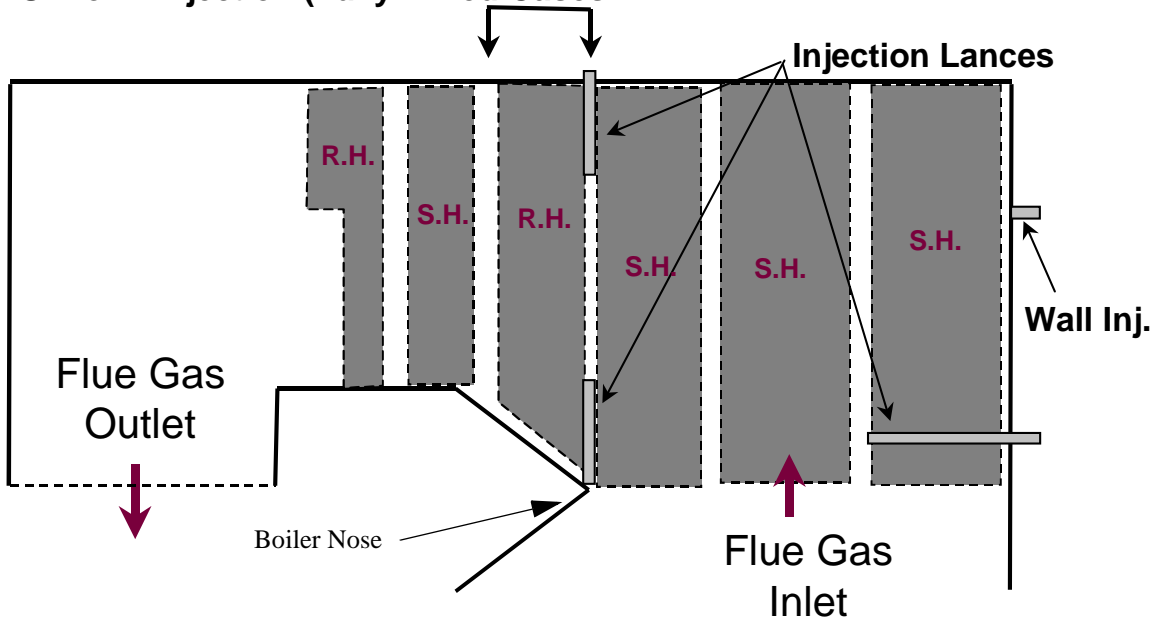


Figure 6-23: Schematic of upper furnace geometry and injection strategies considered in the CFD simulations of Wansley Unit 1. Both lance and wall injection strategies were considered. Convective pass injection was modeled using discrete injectors or by imposing a uniform reagent concentration in the convective pass cavities.

Table 6-4: Predicted NO_x Reduction and NH₃ slip for Wansley Unit 1, NO_{x, in}=310ppm

Strategy	NSR	Avg. NO _x (ppm)	NO _x Reduction (%)	Avg. NH ₃ (ppm)	Max NH ₃ (ppm)
1 (Fully-Mixed Case)	1	259	17	<1	2
2 (Fully-Mixed Case)	1	208	33	<1	6
3 (Floor & Roof Inj.)	1	181	42	90	1330
4 (Lower Wall Inj.)	1	306	1	<1	<1
5 (Wall & Lance Inj.)	1	283	9	<1	1
6 (Upper Wall, Urea)	1	241	22	6	120
7 (Low-Energy, Urea)	1	256	17	15	440

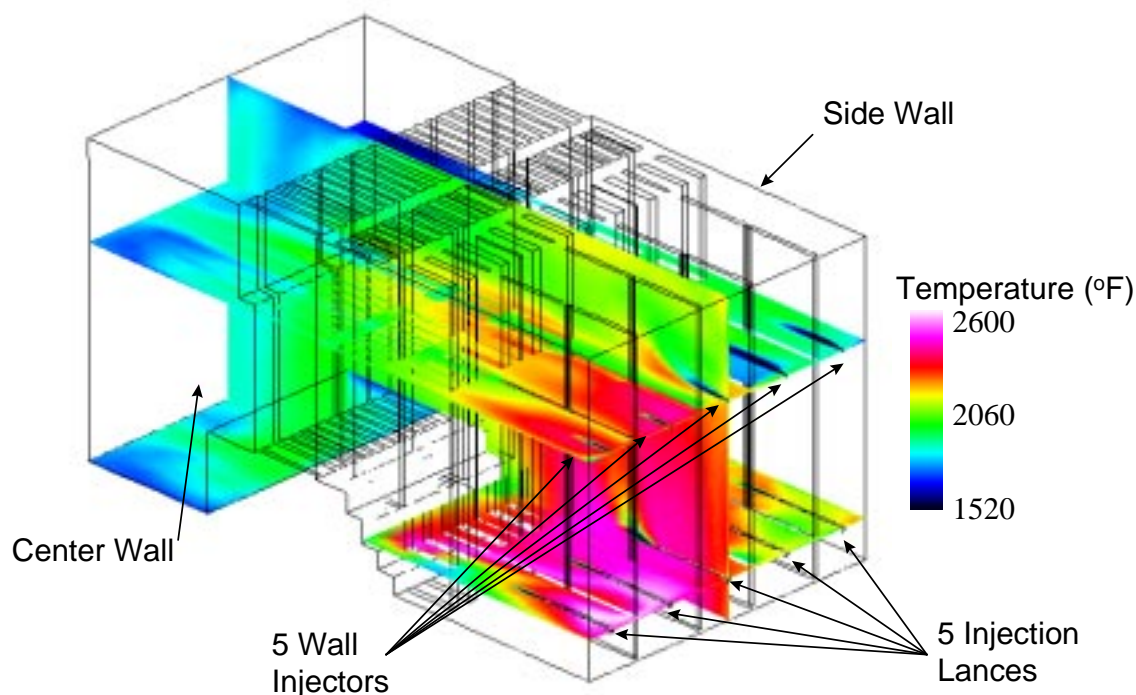


Figure 6-24: Predicted upper furnace temperature distribution for Wansley Unit 1. The particular case shown includes 10 front wall high-energy anhydrous ammonia injectors (Case 5). Horizontal and vertical planes are shown in the vicinity of the injectors to show the local flue gas temperature.

The best strategy in terms of NO_x reduction with low ammonia slip involved the use of high-energy aqueous urea injection from the front wall, which yielded NO_x reduction on the order of 22%.

6.2.3.1 Convective Pass Injection (Fully-Mixed Cases)

Cases 1-3 were investigated to determine the potential for utilizing convective cavity injection in Wansley Unit 1. Cases 1 and 2 assumed uniformly mixed NH₃ in the vertical planes above the tip of the nose and one convective pass cavity downstream of the nose, respectively (Figure 6-25). These cases were performed to determine possible performance of convective cavity injection if reagent could be uniformly mixed in this region. In both of these cases, the NH₃ slip was low (<1 ppm) and NO_x removals were predicted to be 17% and 33%, respectively. Figure 6-26 shows the predicted temperature and NO_x distributions for Case 1. It can be seen that NO_x reduction is maximized in regions where the gas temperatures are favorable for SNCR and reduction is poor in the high temperature regions that are outside the SNCR temperature window.

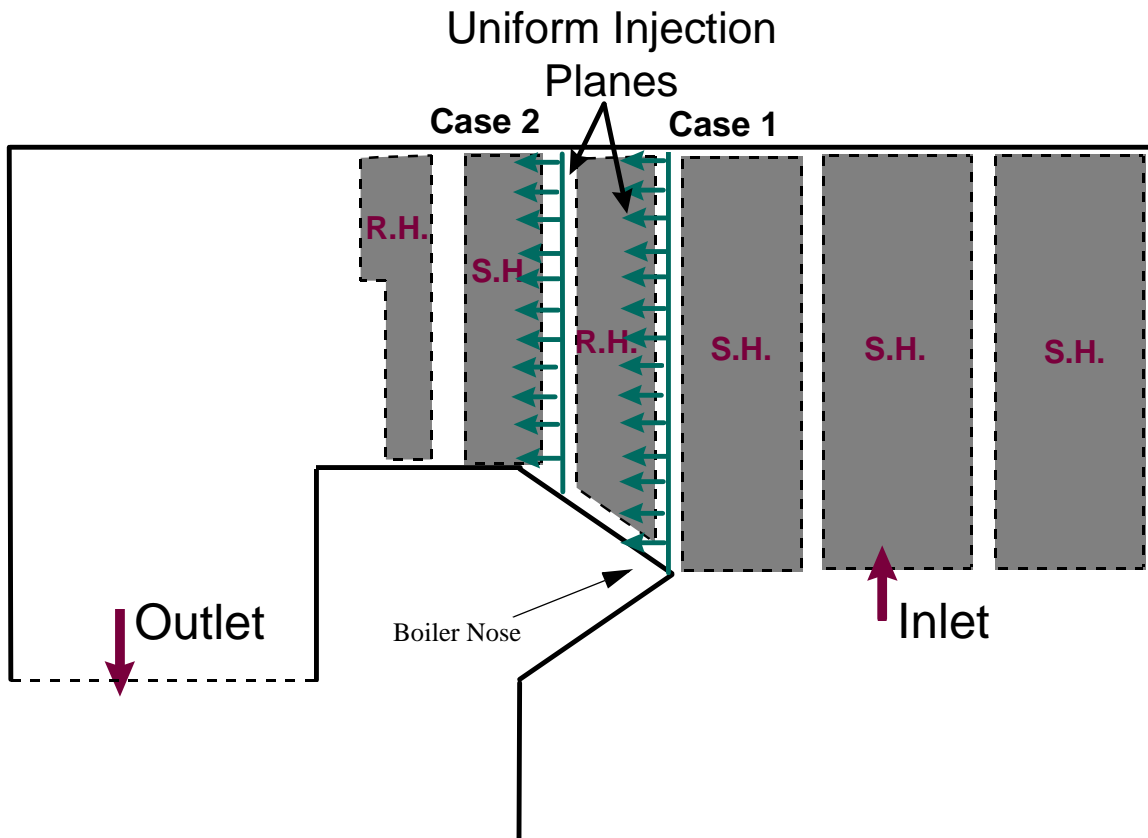


Figure 6-25: Schematic for Wansley Cases 1 and 2 showing location of uniform reagent injection planes. Gaseous NH_3 is assumed to be fully mixed and uniformly distributed in the flue gas at the locations shown here.

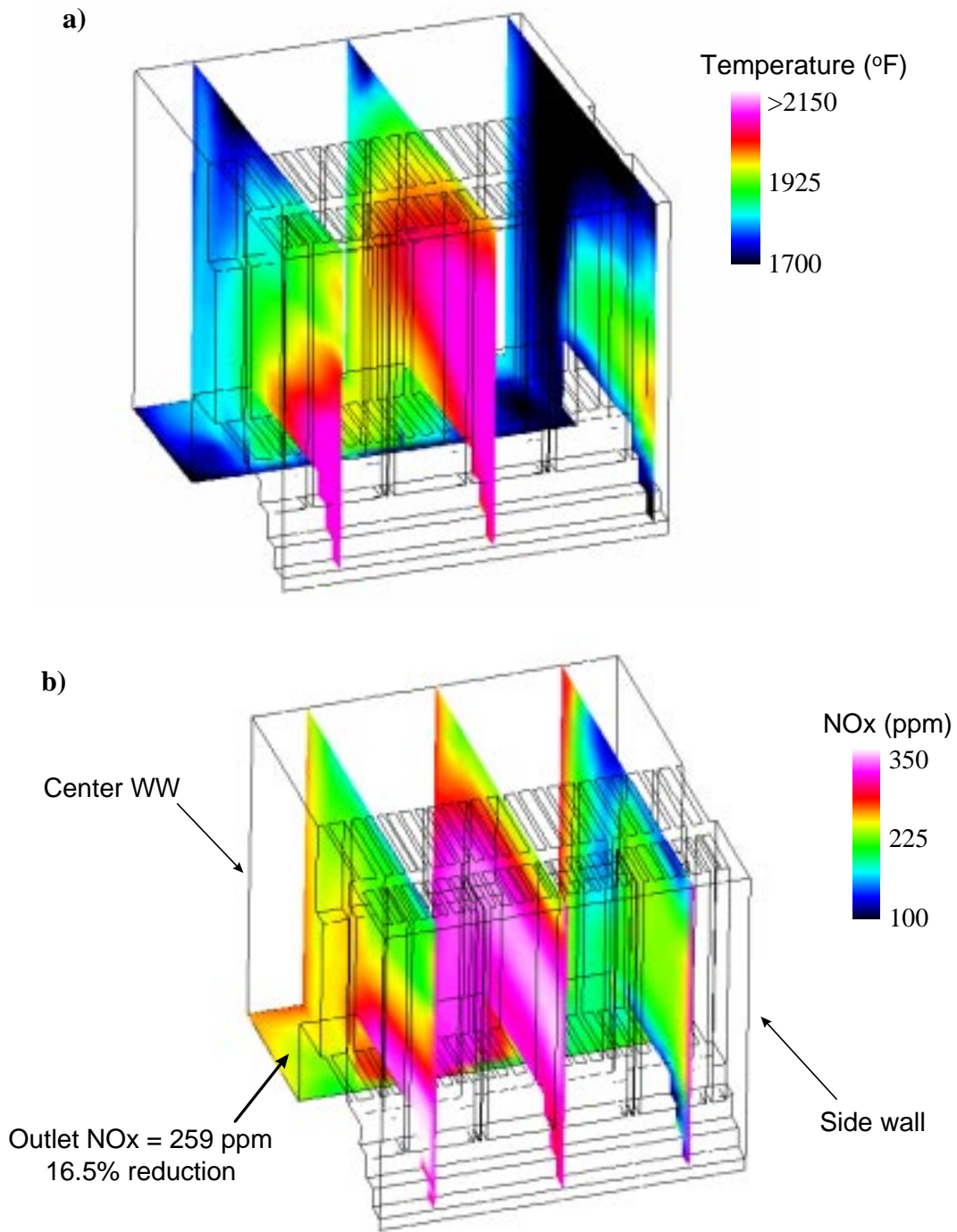


Figure 6-26: Predicted upper furnace temperature and NOx concentration profiles in Wansley Unit 1 Case 1. In this case, NH₃ reagent is uniformly mixed with flue gas in the vertical plane at the nose tip. a) Temperature. b) NOx mole fraction.

Although not shown here, the average ammonia slip for Cases 1 and 2 is low due to the imposition of complete mixing. The gas temperature is not sufficiently low to completely quench the SNCR chemistry to cause significant ammonia slip.

6.2.3.2 High-Energy Anhydrous Ammonia Injection

Since Cases 1 and 2 represent fully-mixed case scenarios and cannot be achieved in practice, Case 3 was considered since it represents a physically realistic, although challenging, design for injection in the convective passes. It involves injectors in the floor and the penthouse in the vertical plane above the tip of the nose (Figure 6-27). A total of ten discrete injectors were placed in the floor and roof, aligned vertically at the tip of the nose, immediately upstream from the first convective pass. The predicted NO_x and NH₃ distribution for this case is shown in Figure 6-28. The favorable temperatures in the region of injection and downstream of it contribute to the good level of NO_x reduction (42%). However, ammonia slip was predicted to be quite high, 90 ppm, due to incomplete mixing. The convective panels in the boiler limit the amount of cross-stream mixing causing highly concentrated lobes of unreacted ammonia. In addition to causing a relatively high average concentration of ammonia at the exit, the predicted distribution was extremely variable. Peak values were as high as 1330 ppm (Table 6-4) in this case due to these mixing limitations. Although the high NH₃ slip potentially could be reduced using additional injectors in this region, maintenance issues related to placement of injectors through the furnace penthouse or nose are a significant concern.

Cases 4 and 5 involved furnace injection further upstream of the convective passes where the flue gases are considerably hotter. Case 4 utilized five front wall injectors at an elevation 5 ft.

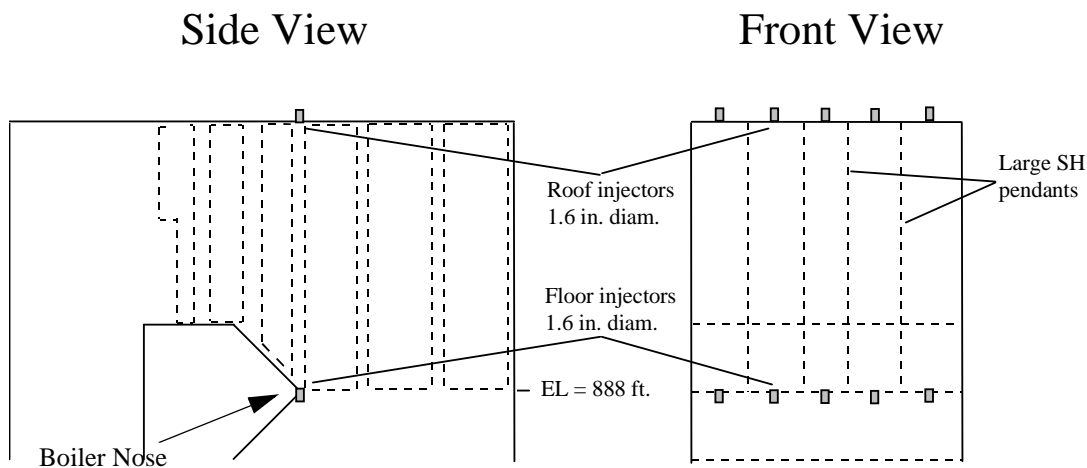


Figure 6-27: Convective pass injection strategy for Wansley Case 3. A total of ten high-energy injectors are placed in the floor and penthouse in the vertical plane at the tip of the nose, centered between the superheater pendants that are directly upstream.

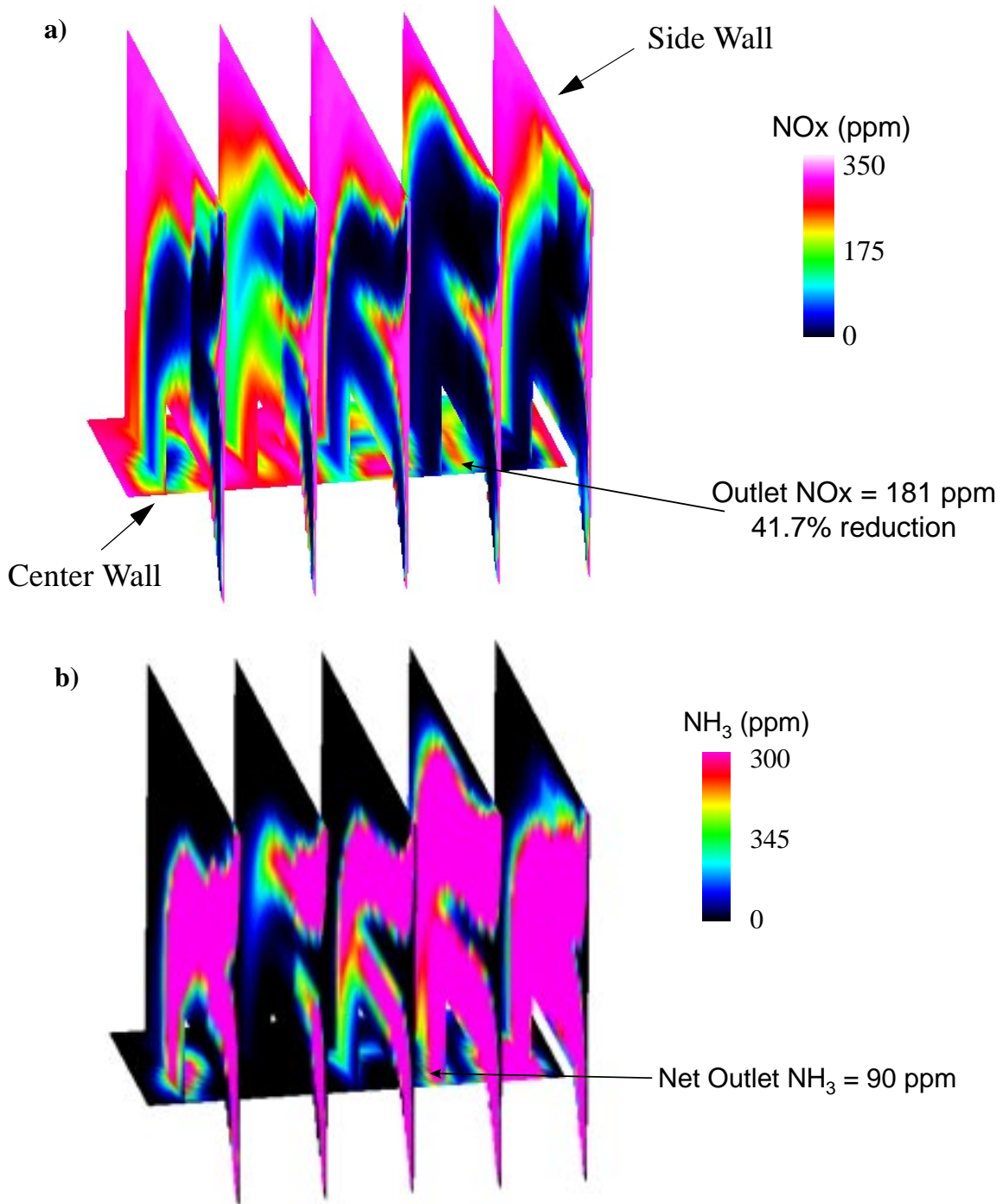


Figure 6-28: Predicted a) NO_x and b) NH₃ distribution for Wansley Case 3 utilizing high-energy anhydrous ammonia injection from floor and penthouse injectors at the tip of the nose. The convective panels limit the degree of lateral mixing resulting in pockets of high slip.

above the tip of the nose (Figure 6-29). Figure 6-30 shows the predicted gas temperature and NO_x distribution for this case. The relatively high flue gas temperature in the region of injection contributes to the extremely low level of predicted overall NO_x reduction (1%). Adjacent to the side wall, the temperatures are predicted to be more optimal, and some significant NO_x reduction is predicted there.

Case 5 involved the use of both lance and front wall injectors (Figure 6-31). Of the strategies that were tested in the physical cold flow modeling, this injection strategy was found to be the best from a mixing standpoint (Martz and Muzio, 1997). The lower level lance injectors efficiently mix reagent into the lower region of the upper furnace while the upper level wall injectors mix reagent into the upper region of the upper furnace. Figure 6-24 shows the gas temperature in the region of the injectors. The gas temperature adjacent to the front wall at the upper elevation where the wall injectors are located is significantly cooler and more optimal for SNCR than at the elevation of the lance injectors. Figure 6-32 shows the predicted NO_x distribution for this case. The more optimal gas temperatures at the upper elevation where the wall injectors are located results in some significant NO_x reduction. However, at the lower elevation where the lances are located, the gas temperature is too hot and little to no NO_x reduction occurs. The result is net NO_x reduction on the order of 9% with ammonia slip less than 1 ppm.

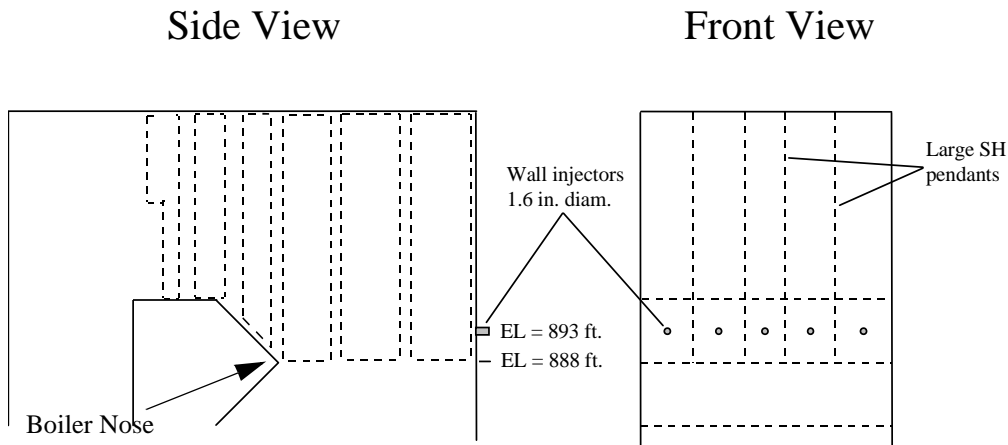


Figure 6-29: Schematic showing injection strategy for Wansley Case 4. Five front wall injectors are centered between the large superheater pendants and are placed at an elevation five feet above the tip of the nose.

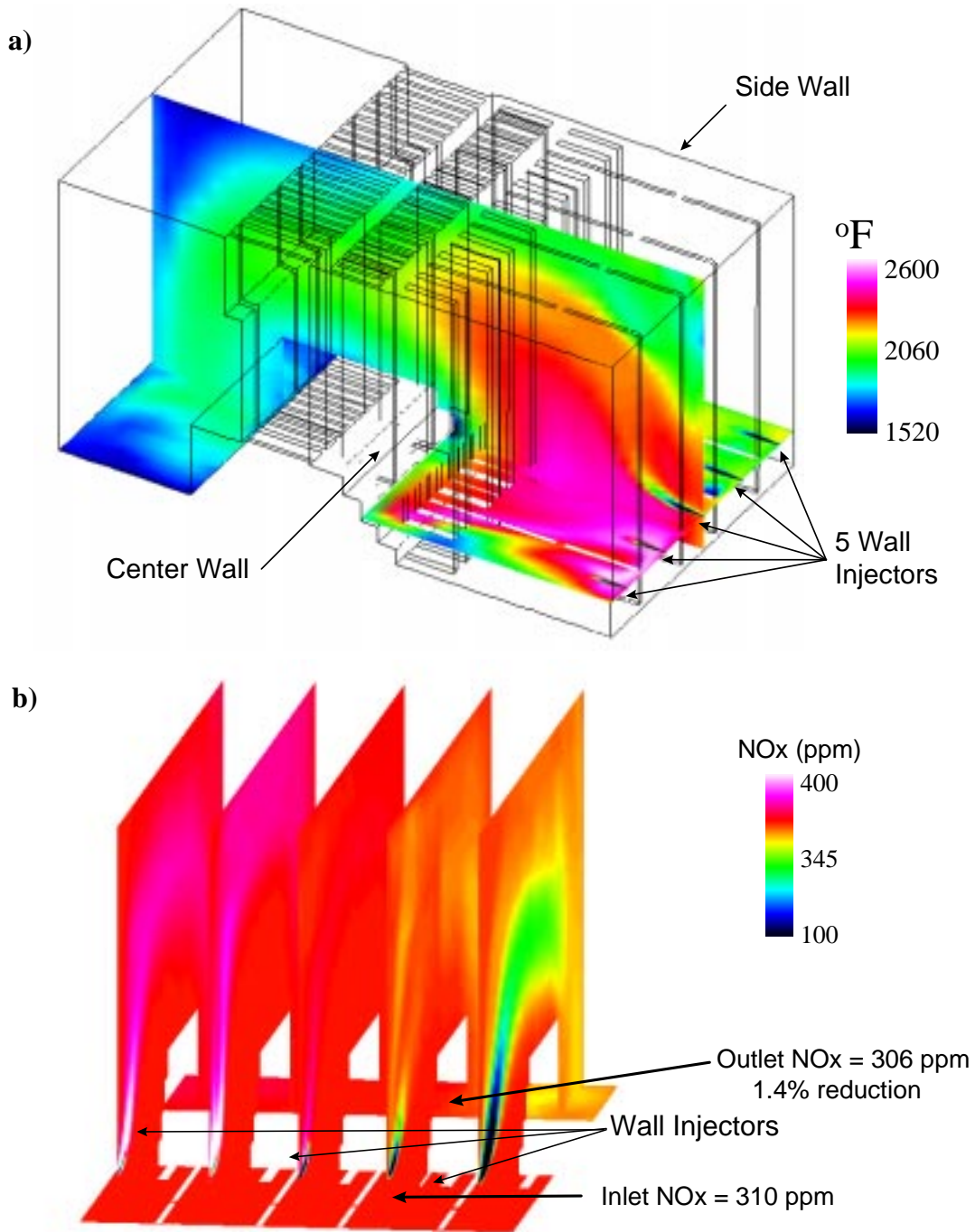


Figure 6-30: Predicted a) temperature and b) NOx distribution in Wansley Case 4. High flue gas temperature in the region of injection result in very low net NOx reduction. Flue gas temperature adjacent to the side wall is predicted to be cooler resulting in significant NOx reduction in this region.

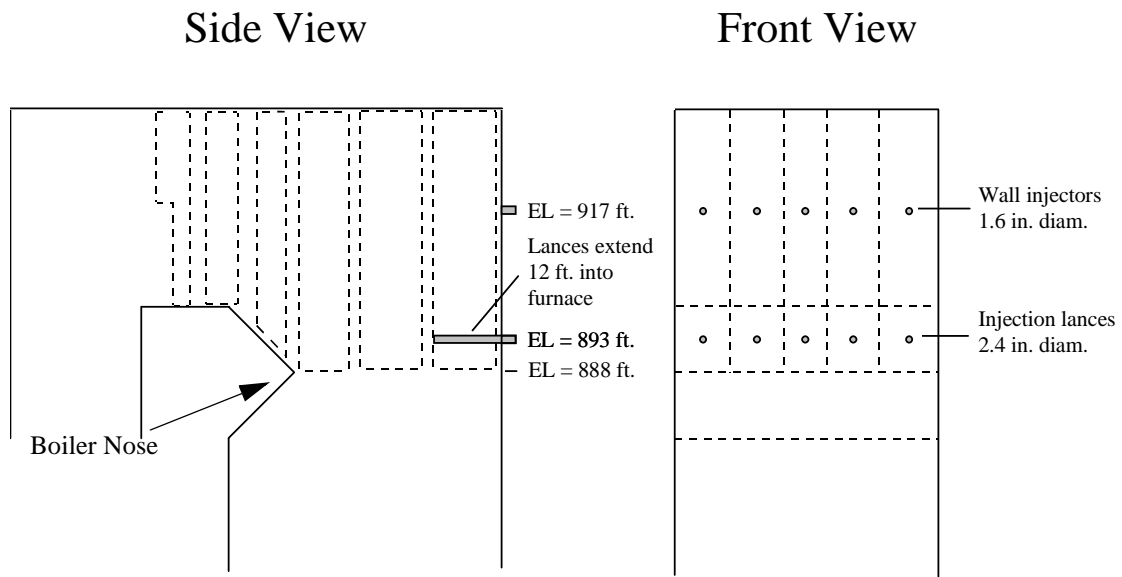


Figure 6-31: Schematic showing injection strategy for Wansley Case 5. Five upper level front wall injectors and five lower level lance injectors are centered between the large superheater pendants.

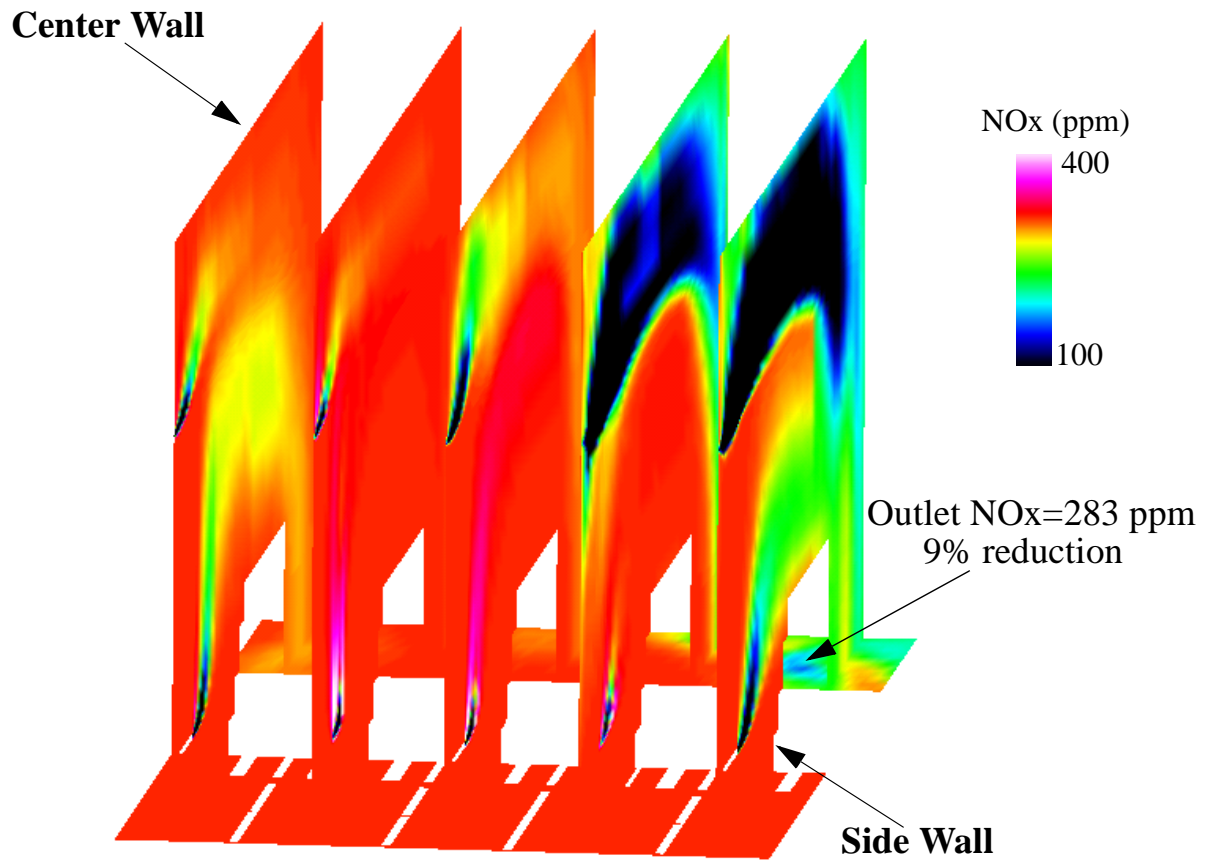


Figure 6-32: Predicted NOx distribution for Wansley Case 5. The upper level wall injectors contribute to more NOx reduction than the lance injectors. The interior lance injectors contribute to NOx formation due to the hot gas temperature in that region.

6.2.3.3 Aqueous Urea Injection

Although none of the cases for Wansley appear to merit a full-scale installation, the best injection strategy considered in the CFD modeling involved aqueous urea injection from the front wall, designated as Case 6 in Table 6-4. This injection strategy is shown schematically in Figure 6-33. Five front-wall injectors were centered between the large superheater pendants adjacent to the front wall at an elevation of 29 feet above the tip of the nose. A 10% aqueous urea solution was used and the spray droplet size distribution, ranging from 8 μm to 195 μm , was assumed to have a Sauter mean diameter of 35 μm .

The predicted temperature and gaseous urea products distribution for this case is shown in Figure 6-34. The gas temperature in the region of the upper level wall injectors is much more suitable for effective SNCR operation than at the lower elevations. However, when the injectors are placed only at this upper level, much of the flue gas is left untreated as is seen in Figure 6-34b.

The droplet chemistry was modeled by requiring that complete evaporation of the water from the droplet had to occur prior to urea particle temperature increase and decomposition into approximately equal parts of NH_3 and HNCO . This delay, before the decomposition products become chemically active in the gas phase, can be seen in Figure 6-35. The concentration of the urea decomposition products (NH_3 and HNCO) peaks downstream of the location where the concentration of water vapor peaks. In reality, reagent will become active in the gas phase, to a small degree, prior to complete evaporation of the water from the droplet. Conceivably,

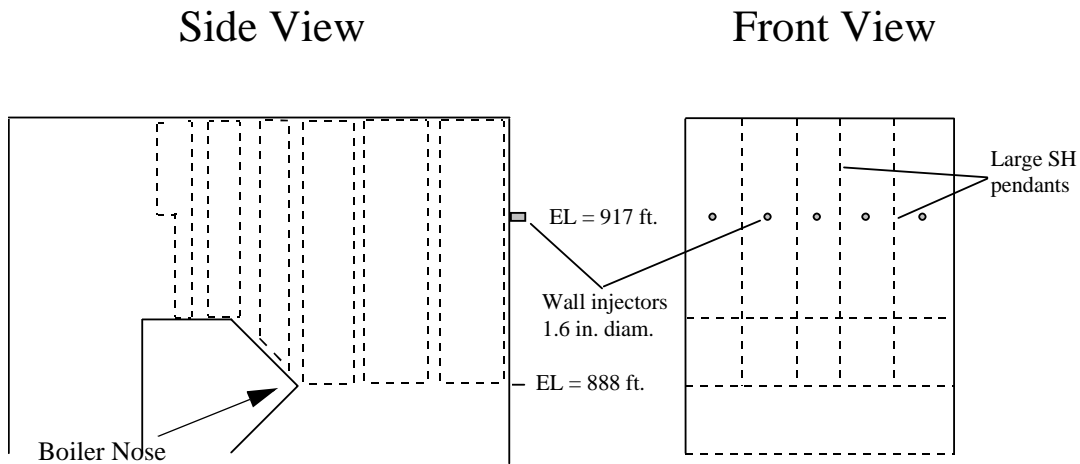


Figure 6-33: Injection strategy for Wansley Case 6. This strategy involves five upper level front wall injectors at an elevation 29 ft. above the furnace nose. Aqueous urea droplets are injected at high-energy.

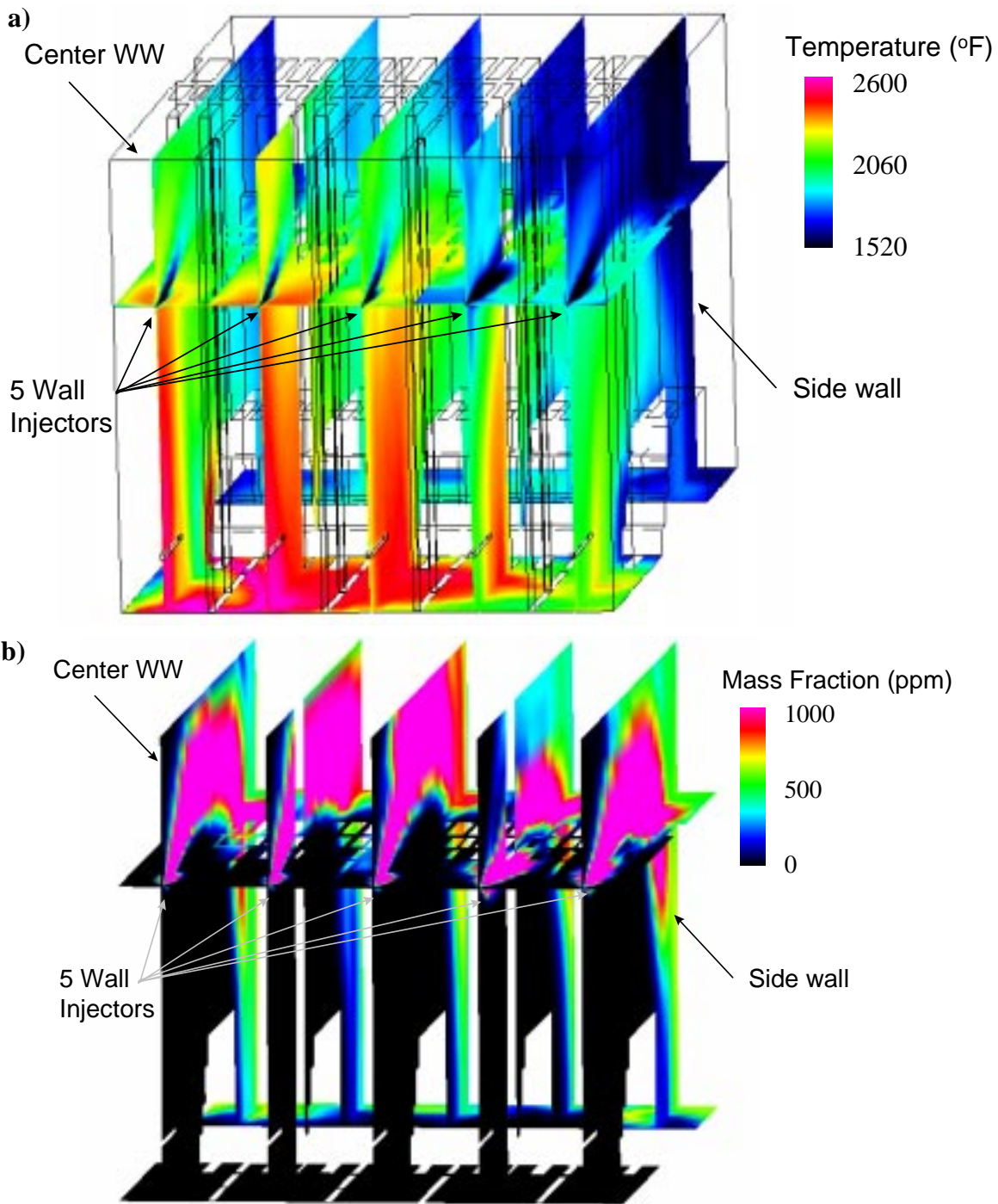


Figure 6-34: Predicted a) gas temperature and b) urea products distribution for Wansley Case 6. Aqueous urea is injected at high-energy through five upper level front wall injectors. The gas temperature at this upper elevation is more suitable for SNCR than at lower levels. Reagent mixing, however, is poor since only the upper level flue gases are treated.

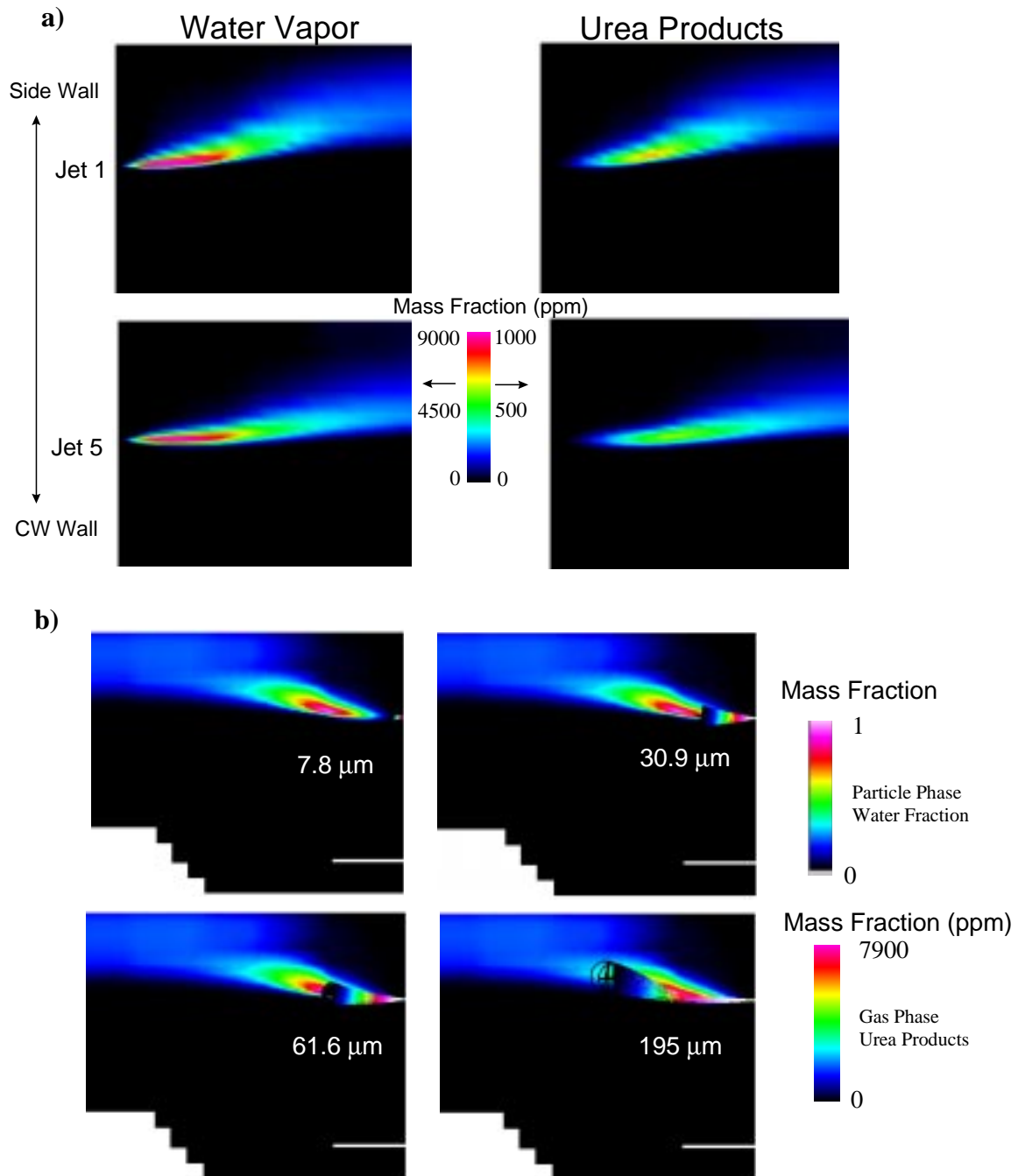


Figure 6-35: a) Gas phase urea products and water vapor from droplets in the plane of two injectors for Wansley Case 6. The water evaporates from the droplets prior to the thermal decomposition of the urea. b) Gas phase urea products and droplet trajectories for four droplet sizes are shown. As expected, it takes longer for the water to completely evaporate from the larger droplets than for the smaller droplets.

this assumption could have a small effect on the predicted NO_x reductions depending on whether the urea products become active in the gas phase where the gas temperature is more optimal or less optimal. Figure 6-35 also shows the effect of droplet size on the droplet trajectory and the time necessary for complete evaporation. NO_x reduction for this case was predicted to be on the order of 22% with 6 ppm NH₃ slip (Figure 6-36). Although the average ammonia slip was predicted to be relatively low in this case, the distribution was again highly variable with peak values as high as 120 ppm (Table 6-4).

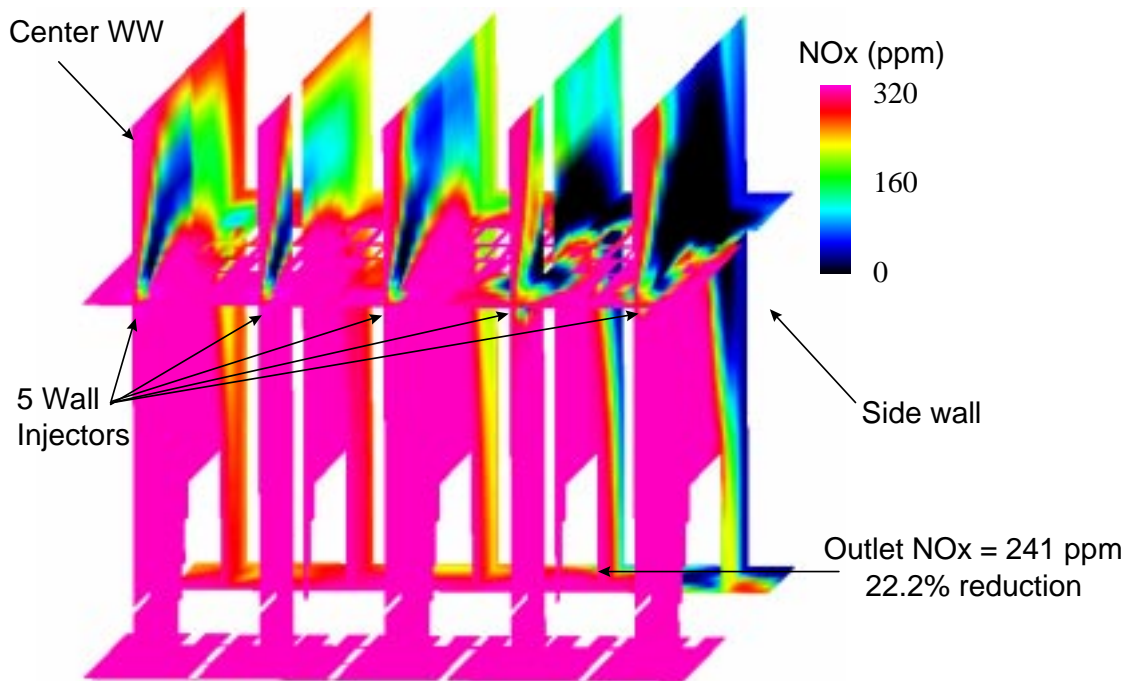


Figure 6-36: Predicted NO_x distribution in the upper furnace for Wansley Case 6 utilizing front wall injection of aqueous urea. NO_x reduction is highest adjacent to the side wall where the gas temperature is more optimal for SNCR.

Case 7 was considered to evaluate the potential of a low-energy aqueous urea injection system that has about double the number of injectors utilized in any of the high-energy systems that were modeled. A schematic of this configuration is shown in Figure 6-37. There are a total of 22 injectors, 20 located at two elevations on the front wall, and 2 located located on the side wall. The front wall injectors are centered on equal areas in the gaps between the large superheater pendants adjacent to the front wall. The droplets were assumed to be 10% urea by weight, to have an initial velocity of 49 ft/sec with a 30° full cone spray angle, and a 100 μm Sauter Mean Diameter (SMD) size distribution. Since the urea droplets are injected at relatively low-energy, they do not penetrate far into the furnace as is shown in Figure 6-38 and comparing with Figure 6-35. As a result, overall mixing of the reagent (urea decomposition products) is limited as is seen in Figure 6-39. The overall NO_x reduction for this case was predicted to be 17% with 15 ppm ammonia slip. The predicted NO_x distribution for this case is shown in Figure 6-40. Much of the unreacted ammonia is located adjacent to the side wall where the gas temperature is cooler and additional reagent is injected from the side wall.

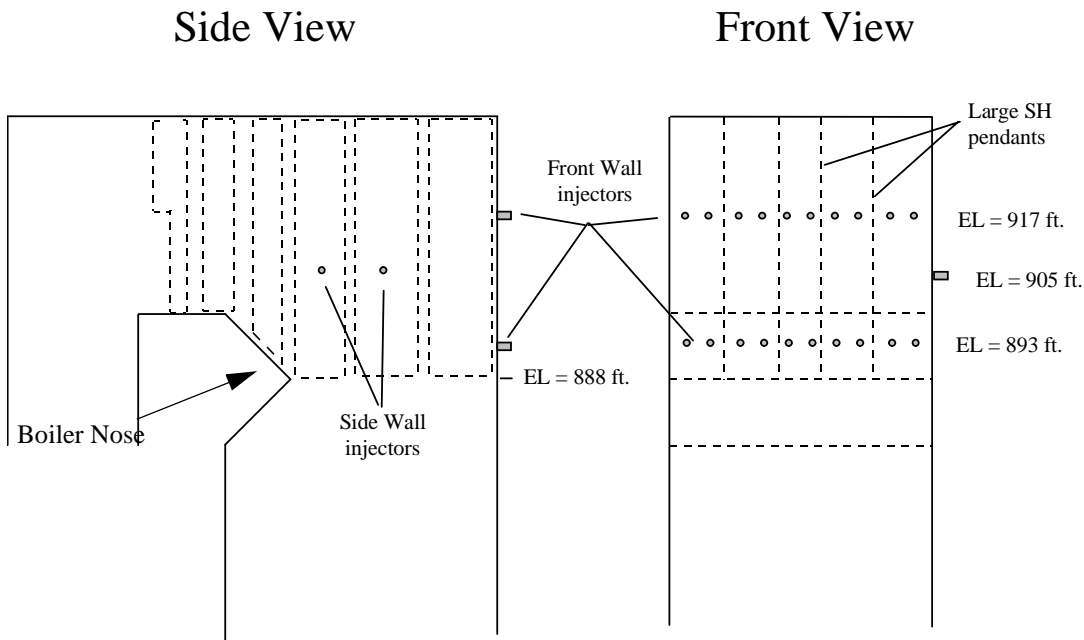


Figure 6-37: Injection strategy for Wansley Case 7. This strategy involves low-energy aqueous urea injection utilizing 22 injector locations. Front wall injectors are located at two elevations with 10 injectors at each elevation. Two side wall injectors are placed at two downstream locations as shown.

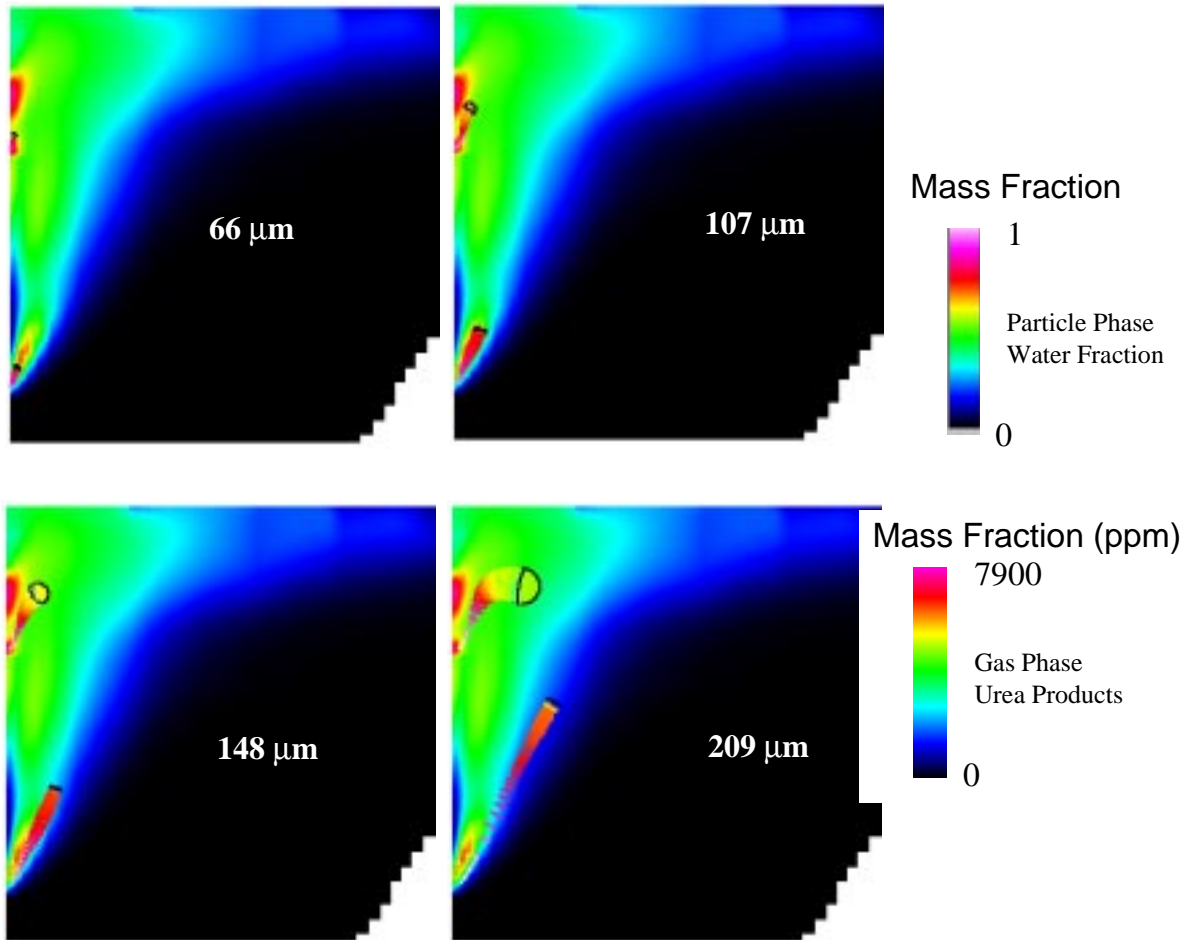


Figure 6-38: Predicted distribution of urea gas phase products and mean droplet trajectories for four droplet sizes for Wansley Case 7. The trajectories are colored by the mass fraction of water remaining in the droplet. The trajectory terminates when there is no mass (water and urea) remaining in the droplet. Droplet penetration into the furnace is relatively small in comparison with high-energy injection in Case 6.

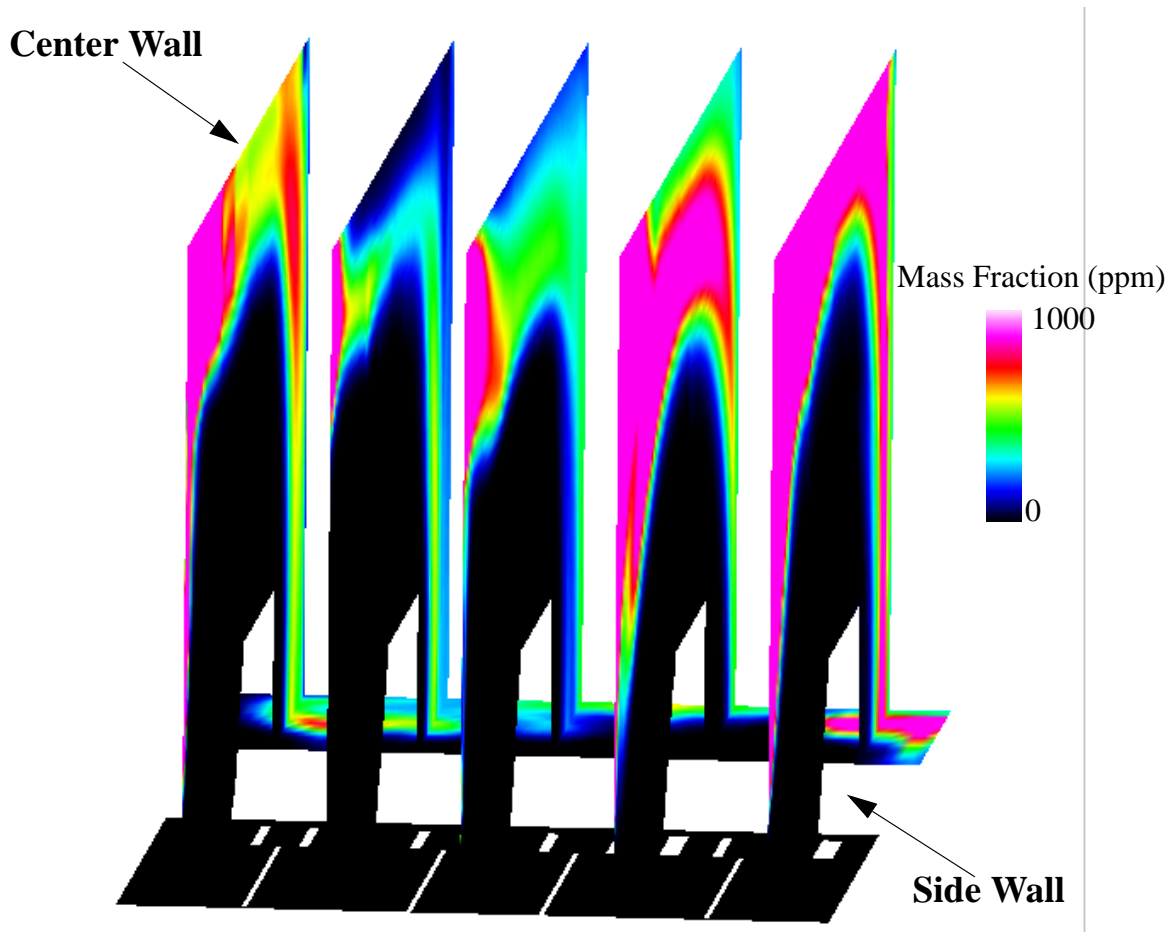


Figure 6-39: Mass fraction of urea gas phase products for Wansley Case 7. Only the upper level flue gas is treated since the injected reagent droplets do not penetrate very far into the furnace. Reagent concentration is high adjacent to the side wall due to the extra side wall injectors.

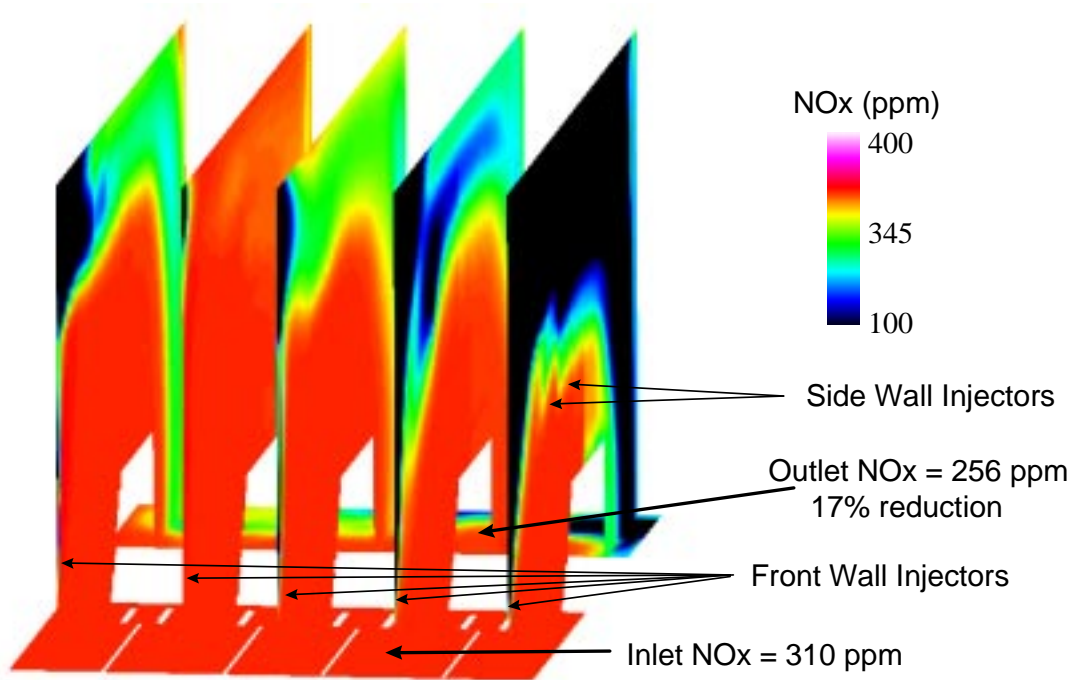


Figure 6-40: Predicted NOx distribution for Wansley Case 7 involving low-energy aqueous urea injection. Poor penetration of reagent into the furnace results in limited mixing of reagent with the lower level flue gas. The side wall injectors contribute to significant NOx reduction in the region adjacent to the side wall, but incomplete mixing and cooler temperatures there cause high localized ammonia slip.

6.2.3.4 Summary of Wansley Unit 1 Predictions

None of the injection strategies considered for Wansley Unit 1 appear to merit a full-scale installation. Under full load operation, gas temperatures near the furnace exit are too hot for effective SNCR. Injection strategies involving a combination of front wall injectors and 12 ft. long lances inserted through the front wall (Case 5), that are optimal from a standpoint of mixing, yield very limited NO_x reduction due to the high temperatures. Installation of furnace lances to accommodate convective pass injection in this boiler is difficult due to the existence of a center waterwall. The convective pass injection scenario considered in the CFD modeling (Case 3) indicated that injection only through the floor and penthouse in the convective pass region above the nose is problematic primarily due to poor mixing between the injected reagent and the flue gas. This case resulted in pockets of high concentrations of unreacted ammonia. Boilers that can more easily accommodate the installation of furnace lances within the convective section, to be used in combination with upper level front wall injectors, could possibly see better SNCR performance than predicted for this particular boiler. The best of the strategies considered, involved high-energy injection of aqueous ammonia from upper level front wall injectors (Case 6). For NSR=1, NO_x reduction was 22% with 6 ppm ammonia slip. Low-energy injection of aqueous urea from more than double the number of injectors resulted in lower NO_x reduction and higher ammonia slip than the high-energy case.

7.0 CONCLUSIONS

The SNCR systems evaluated in this program were designed for full load steady state operations only. (For example, multiple levels of wall injectors or rotating furnace lances would be required to adequately follow cycling operations and changing boiler conditions.) In addition, SNCR performance is site specific. As a result, caution should be taken in applying these results to day-to-day operations over a range of boilers, with various boiler duty cycles and swinging loads.

For the wall-fired unit equipped with low-NO_x burners and overfire air (Hammond Unit 4), the results showed that SNCR has the potential to reduce NO_x emissions by up to 30-35 percent while maintaining ammonia slip below 5 ppm. Of the configurations evaluated, the most promising scenario involved the injection of ammonia (NSR = 1.0) via a row of high-energy wall injectors located on the front wall 14 feet above the tip of the nose. The improvement in NO_x reduction at higher NSRs was seen to be relatively small.

For the tangentially fired unit equipped with a low-NO_x concentric firing system (Wansley Unit 1), the results showed that SNCR has the potential to reduce NO_x emissions by 20-25 percent with an ammonia slip less than 10 ppm. Of the configurations evaluated, the most promising scenario involved the injection of aqueous urea via high-energy wall injectors located on the front wall 29 feet above the tip of the nose. The firing characteristics of this boiler (supercritical, separated overfire air, eastern bituminous fuel, 8 corner) make achieving higher levels of NO_x reduction difficult. The most influential factor is the separated overfire air system, which elevates upper furnace temperatures by causing the combustion process to extend beyond the furnace nose and into the convection section.

For both units considered in this study, the high furnace exit gas temperatures led to the use of upper level front wall injectors. However, relatively poor mixing of reagent is achieved by using front wall injection alone. Upper level front wall injection combined with lower level multi-nozzle lances in the convective pass region appears to be a good strategy from a mixing standpoint. However, in this study, the tangentially fired unit did not provide access for sidewall lances due to the center waterwall, making the placement of lances in the convective pass region difficult. In other units without this constraint, SNCR performance could be better. Due to site specific characteristics like this, care should be taken in extrapolating these results to all other large coal-fired boilers. SNCR performance could be better or worse than was found for the two units evaluated here.

For every case evaluated, ammonia slip levels at the model exit were highly variable. In many cases, the peak ammonia slip was more than an order of magnitude higher than the average ammonia slip. For example, if the average ammonia slip was 6 ppm, the peak ammonia slip was at least 60 ppm. Although limited to a small region of the total exit area, the impact of such a high ammonia concentration could result in localized pluggage of an annular region of the air heater as it rotates through the high slip zone. However, in practice, tuning individual nozzle flow rates could help to reduce these high localized slip levels.

8.0 REFERENCES

- Adams, B. R., "Computational evaluation of mechanisms affecting radiation in gas and coal fired industrial furnaces," Ph.D. Dissertation, Department of Mechanical Engineering, University of Utah, (1993).
- Adams, B. R., and Smith, P. J., "Three-Dimensional discrete-ordinates modeling of radiative transfer in a geometrically complex furnace," *Combust. Sci. and Tech.*, **88**, 293 (1993).
- Adams, B. R., and Smith, P. J., "Modeling effects of soot and turbulence-radiation coupling on radiative transfer in turbulent gaseous combustion," *Combust. Sci. and Tech.*, **109**, 121 (1995).
- Bockelie, M.J., Adams, B.R., Eddings, E.G., and Smith, P.J., "Simulations of High Temperature Reacting Flows For Industrial Processes," Numerical Grid Generation in Computational Field Simulations, published by the MSU NSF-ERC for Computational Field Simulations, Mississippi State University, Starkville, MS, April, 1996, pp. 913-922.
- Bockelie, M.J., Adams, B.R., Cremer, M.A., Davis, K.A., Eddings, E.G., Valentine, J.R., and Smith, P.J., "Computational simulations of industrial furnaces," submitted for presentation at the Int'l Symp. on Computational Technologies For Fluid/Chemical Systems with Industrial Applications, Joint ASME/JSME Conference, San Diego, CA, July, 1998.
- Brouwer, J., Heap, M., Pershing, D., and Smith, P., "A Model for Prediction of Selective Non-catalytic Reduction of Nitrogen Oxides by Ammonia, Urea, and Cyanuric Acid with Mixing Limitations in the Presence of CO," Twenty-Sixth Symposium (International) on Combustion, The Combustion Institute, 1996.
- Brouwer, J., Bockelie, M.J., Davis, K.A., Heap, M.P., Pershing, D.W., and Beittel, R. "Analysis of low emission firing systems for a slag tap low emissions boiler system," "International Joint Power Generation Conference, ASME, October, 1996.
- Cremer, M.A., Adams, B.R., Heap, M.P., Smith, P.J., and Brown, D.J., "Improving the Performance of Process Heaters through Fireside Modeling," AFRC 1997 International Symposium, September, 1997
- Davis, K.A., Bockelie, M.J., Smith, P.J., Heap, M.P., Hurt, R.H., and Klewicki, J.P., "Optimized Fuel Injector Design for Maximum In-Furnace NO_x Reduction and Minimum Unburned Carbon," Proceedings of the First Joint Power and Fuel Systems Contractors Conference, DOE-PETC, Pittsburgh, PA, July 9-11, 1996.
- Dean, A.J., Hanson, R.K., and Bowman, C.T., *J. Phys. Chem.* **95**, 3180-3189, 1991.
-

Eddings, E.G., Davis, K.A., Heap, M.P., Valentine, J.R., Facchiano, A., Hardman, R., and Grigas, N., "Effect of Low-NO_x Firing Conditions on Increased Carbon in Ash and Water Wall Corrosion Rates," The Mega Symposium: EPRI-DOE-EPA Combined Utility Air Pollutant Control Symposium, August 1997.

Institute of Clean Air Companies (ICAC), SNCR Committee, Selective Non-Catalytic Reduction (SNCR) for Controlling NO_x Emissions, July 1994.

Lin, Chin-I, "Full Scale Tests of SNCR Technology on a Gas-Fired Boiler", EPRI Workshop on NO_x Controls for Utility Boilers, July 1992.

Martz, T.D., and Muzio, L.J., "Physical Flow Modeling Report-Large Scale SNCR Project," Prepared for Southern Company Services, December 1997.

Miller, J.A. and Bowman, C.T., "Mechanism and Modeling of Nitrogen Chemistry in Combustion," Prog. Energy Combust. Sci. 15, 287-338, 1989.

Patankar, S.V., Numerical Heat Transfer and Fluid Flow, Hemisphere Publishing Corp., Washington, D.C., 1980.

Science Applications International Corporation (SAIC), Performance of Group 2 Boiler NO_x Control Technologies, August 1996.

Shore, D., et al, "Urea SNCR Demonstration at Long Island Lighting Company's Port Jefferson Station, Unit 3", Proceedings of the EPRI/EPA Joint Symposium on Stationary Combustion NO_x Control, May 1993.

Smith, L.L. and Larsen, L.L., "500 MW Demonstration of Advanced Wall-Fired Combustion Techniques for the Reduction of Nitrogen Oxides (NO_x) Emissions from Coal-Fired Boilers," Innovative Clean Coal Technology Program Topical Report, 1993.

Smoot, L.D. and Smith, P.J., Coal Combustion and Gasification, Plenum Press, New York, 1985.
